

SPEAKER ABSTRACTS

1. Pore Planning: Functional Membrane Proteins by Design HAGAN BAYLEY, *Department of Medical Biochemistry & Genetics, The Texas A&M University, System Health Science Center, College Station, Texas 77843-1114*

My laboratory has used genetic engineering and targeted chemical modification to produce functionalized pore-forming proteins. The primary target of our studies has been staphylococcal α -hemolysin, which is a 293 amino acid, water-soluble polypeptide that self assembles in lipid bilayers to form heptameric transmembrane pores. We have made α -hemolysins in which pore activity can be triggered or switched on and off by biochemical, chemical, or physical stimuli, including the action of enzymes, noncovalent and covalent modification, and irradiation with near UV light. Recently, the use of noncovalent adapters to modify the properties of the α -hemolysin pore has proved very fruitful. Adapters such as cyclodextrins have been used to change the pore's conductance, ion selectivity, and susceptibility to blockers. We have also initiated studies aimed at producing functional membrane proteins by de novo design. Early results show that the transmembrane β barrel of α -hemolysin has a surprising ability to accommodate new sequences. Engineered protein pores may have applications in biotechnology and they are being tested for their ability to attack malignant cells, to control drug release from particles such as liposomes, and as components of biosensors.

2. Crystal Structure of the Outer Membrane Active Transporter FepA from *Escherichia coli* SUSAN K. BUCHANAN,*§ BARBARA S. SMITH,* LALITHA VENKATRAMANI,† DI XIA,* LOTHAR ESSER,* MAYA PALNITKAR,* RANJAN CHAKRABORTY,† DICK VANDER HELM,† and JOHANN DEISENHOFER,‡ **Howard Hughes Medical Institute and Department of Biochemistry, University of Texas Southwestern Medical Center, Dallas, Texas; and †Department of Chemistry and Biochemistry, University of Oklahoma, Norman, Oklahoma*

Ferric enterobactin receptor (FepA) is an 80 kD outer membrane protein from *E. coli* that binds ferric enterobactin (719 D) and transports it into the periplasm; it also serves as the receptor for colicins B (54.7 kD) and D (74.7 kD). FepA belongs to the family of high affinity, active transport receptors that require proton motive force and TonB-ExbB-ExbD, an integral inner membrane protein complex, to specifically transport iron chelates

and vitamin B12 across the outer membrane. The structure of FepA has been solved at 2.4-Å resolution by multiwavelength anomalous diffraction (MAD) on selenomethionine-containing crystals. Two distinct functional domains are revealed: (a) a 22-stranded beta barrel spans the outer membrane and contains large extracellular loops that appear to function in ligand binding, and (b) a globular NH₂-terminal domain folds into the barrel pore, inhibiting access to the periplasm and contributing two additional loops for potential ligand binding. We infer from the structure that the beta barrel functions primarily as a scaffold, while the NH₂-terminal domain carries out the functions of ligand recognition, transmembrane signaling to the TonB complex, and conformational changes allowing transport into the periplasm. (Supported by a postdoctoral fellowship from the American Cancer Society to S.K. Buchanan and by the Howard Hughes Medical Institute.)

3. From Passive Diffusion to Active Transport Across the Bacterial Outer Membrane, a Structural View W. WELTE, *University of Konstanz, Konstanz, Germany*

Gram-negative bacteria protect their vulnerable cytoplasmic membrane (CM) by a peptidoglycan layer and an outer membrane (OM). Transport across the CM is performed by high-affinity primary and secondary active transport through transporters with K_m values in the μ M range. Near the periplasmic binding sites, the concentration of the molecules transported by these complexes is therefore of a similar order of magnitude. In the absence of the chemiosmotic gradient and ATP, diffusion down this gradient is the only means of transportation across the OM. Fick's equation relates the difference in concentration of a species of molecules in the external space and in the periplasmic space with their flux Φ across the OM: $\Delta c \cdot P = \Phi$. As long as the concentration of nutrient molecules in the culture medium is significantly higher than in the periplasm near the transporters, the diffusive flux Φ can meet the requirements for unhindered cell growth. The permeability P of the OM under such conditions is due to the "general diffusion porins," the major protein component of the OM. They form waterfilled channels for ions and small molecules, smaller than the exclusion limit of the channels (usually 600 D). These porins are 16 stranded antiparallel β -barrels having masses between 30 and 35 kD and form trimers.

When the concentration of essential nutrient molecules drops so that the flux Φ is not sufficient for unhindered growth, the cells are under selective pressure to increase the permeability. In this

situation, the flux depends on the rate constant for entrance into the channel, which is determined by the activation free-energy ΔG^* of the entry process: $k_{\text{ent}} = kBT/h \exp[-\Delta G^*/RT]$. The entropy term $-T\Delta S^*$ will represent a considerable fraction of the free-energy barrier, as the permeating molecules are confined to the narrow cross-section of the channel. Thus the permeability can be increased by introducing binding sites with negative ΔH for a certain nutrient molecule or class of molecules as, for example, sugars or nucleotides into the channel wall. This is the basic mechanism of "specific porins." Two examples are Maltoporin and Sucrose porin (ScrY), which are basically 18-stranded barrels with a chain of low-affinity glucosyl binding sites ("greasy slide") extending on the inside of the barrel wall from the external entrance to the periplasmic exit.

With lower concentration in the external medium, the affinity of the binding sites must be increased to achieve a sufficient rate of entrance. As the sites should not be clogged up by ligands, the high energy of binding must be overcome by a supply of free energy in a subsequent reaction, which means that the cell must use an active transport mechanism.

An example is uptake of ferric iron through the OM. To acquire the virtually insoluble ferric iron from its environment, bacteria and fungi secrete siderophores, small molecules with a mass between 600 and 900 D (e.g., ferrichrome, $M_R = 763$, a derivative of cyclic hexaglycine with three hydroxamate groups that provides an octahedral coordination site). Bacteria possess a special class of outer membrane receptors with a high-affinity binding site near the external surface of the cell to capture siderophore-iron complexes ($K_d = 0.5 \times 10^{-7}$ M) and to transport it across the OM. It was shown that the energy needed to dissociate the siderophore ligand from this site is taken from the chemiosmotic gradient and transduced to the receptors by TonB, a 26-kD protein spanning the cytoplasmic membrane and the periplasmic space. After binding to the periplasmic surface of the receptor, the siderophore is released into the periplasm.

We present here the structure of FhuA, the ferrichrome receptor from *Escherichia coli*, which consists of a 22-stranded barrel domain and an NH_2 -terminal "cork domain" stuffed into the barrel. The structure was determined in complex with and without ferrichrome. In both conformations, the barrel cross-section is blocked for passage of even small molecules. An induced-fit mechanism contracts the barrel wall and the cork domain around the bound ferrichrome near the external opening of the receptor. This conformational change is transduced through the cork domain to the periplasmic side and results in a conspicuous allosteric helix-coil transition at the NH_2 -terminal, periplasmically exposed surface. This may serve to signal the loading state to TonB, ensuring economic use of chemiosmotic energy.

Fungi exploit this ferrichrome uptake mechanism to smuggle antibiotic conjugates as "Trojan horses" into the cytoplasm of their fellow cells. The crystal structure of the albomycin~FhuA complex shows that its hydroxamate moiety is bound to FhuA virtually identically, as in the ferrichrome~FhuA complex.

The crystal structure of FhuA shows a tightly bound lipopolysaccharide (endotoxin) molecule.

4. Structural Studies of MscL, a Gated Mechanosensitive Ion Channel ROBERT H. SPENCER, RANDAL B. BASS, GEOFF CHANG, and DOUGLAS C. REES, *Division of Chemistry, Howard Hughes Medical Institute, California Institute of Technology, Pasadena, California*

Mechanosensitive ion channels are membrane proteins that

open and close in response to mechanical stress applied to the bilayer. The MscL family of mechanosensitive channels is found in prokaryotes and may help regulate osmotic pressure changes within the cell. The structure of the MscL homologue from *M. tuberculosis* has been determined by x-ray crystallography to 3.5-Å resolution to provide a structural framework for understanding channel gating. This channel is organized as a homopentamer, with each subunit containing two transmembrane helices and a third cytoplasmic helix. From the extracellular side, an ~15-Å-diameter opening leads into a pore that narrows to an occluded hydrophobic apex that may act as the channel gate. Similarities with other channels are evident, including the packing of helices to form the permeation pathway, the likely movement of the inner helices as part of the gating mechanism, and the presence of extramembrane domains adjacent to the permeation pathway through the membrane. Implications of the MscL structure for the gating mechanism that couples protein conformation and membrane stretching will be discussed.

5. Nicotinic Acetylcholine Receptor: Structure and Mechanism NIGEL UNWIN, *Medical Research Council, Laboratory of Molecular Biology, Hills Road, Cambridge, United Kingdom*

The nicotinic acetylcholine (ACh) receptor is a cation-selective neurotransmitter-gated ion channel. We are investigating its structure and mode of action by electron microscopy of tubular receptor crystals grown from *Torpedo* postsynaptic membranes. Earlier three-dimensional analyses of the receptor in the closed- and open-channel forms (Unwin, N. 1993. *J. Mol. Biol.* 229:1101–1124; Unwin, N. 1995. *Nature.* 373:37–43) had suggested that the channel is activated by binding of ACh to pockets within the extracellular domains of the α subunits. Binding at the two sites appeared to initiate small rotations of the subunits, triggering a change in configuration of the pore-lining M2 segments, thereby opening up a continuous ion-conducting path across the membrane. The emerging picture, now at near-atomic resolution (Miyazawa et al. 1999. *J. Mol. Biol.* 288:765–786), appears to confirm the essential elements of this mechanism and suggests that electrostatic interactions play an important role in selectively guiding cations towards and away from the membrane-spanning pore.

6. Aquaporin Water Channel Proteins PETER AGRE,* ANDREAS ENGEL,† and YOSHINORI FUJIYOSHI,‡ **Johns Hopkins University School of Medicine, Department of Biological Chemistry, Baltimore, Maryland; †M.E. Müller Institute Bio-center, University of Basel, Basel, Switzerland; and ‡Department of Biophysics, University of Kyoto, Kyoto Japan*

The high water permeability of certain biological membranes is due to the presence of aquaporins, a family of membrane water channels found throughout nature. AQP1 is recognized to be a constitutively active pore that is freely permeated by water when driven by osmotic gradients ($E_a = 4$ kcal/mol) and is inhibited by Hg^{2+} . The inability of this protein to permit transport of larger uncharged solutes is believed to result from the narrowness of the pore (predicted to be 3 Å in diameter), whereas the inability to permit transport of protons (H_3O^+) is yet unexplained. Molecular genetic studies predicted the subunit to have six bilayer-spanning α -helices comprised of tandem repeats, each having three bilayer spans oriented in obverse symmetry. The two most highly conserved domains are loop B, which separates TM2 and TM3, and

loop E, which separates TM5 and TM6. These elements contain the signature motive Asn-Pro-Ala (NPA) that are found in all homologues. Loops B and E were predicted to fold into the lipid bilayer from the intracellular and extracellular leaflets, creating a single transmembrane pore referred to as the "hourglass." Studies of native and expressed aquaporin proteins demonstrated that the functional unit is a homotetramer containing four independent aqueous pores. Cryoelectron microscopic analyses have now solved the structure to $<4.5 \text{ \AA}$, revealing the location of the Hg^{2+} binding site and key intra- and intersubunit associations. Membrane crystals containing other aquaporin homologs with varying selectivity to solutes are revealing structural variations to the tetrameric hourglass assembly. Together, these studies have provided an atomic model for the AQP1 protein and are defining the molecular basis of membrane water transport.

7. Structure and Mechanisms of Respiratory Chain Complexes CAROLA HUNTE, C. ROY, D. LANCASTER, and HARTMUT MICHEL, *Max-Planck-Institut für Biophysik, Frankfurt, Germany*

The respiratory chain of mitochondria and many aerobic bacteria consists of an NADH dehydrogenase (complex I), succinate dehydrogenase (complex II), the cytochrome b_6 -complex (complex III), and cytochrome c oxidase (complex IV). To understand their mechanisms of action, we have recently crystallized the complex II-like fumarate reductase from the bacterium *Wolinella succinogenes*, the cytochrome b_6 -complex from yeast, and the cytochrome c oxidase from the soil bacterium *Paracoccus denitrificans*.

Fumarate reductase from *W. succinogenes* oxidizes menadiol and reduces fumarate, the product is succinate. It consists of an FAD containing subunit A, which contains the site of fumarate reduction, three Fe/S-clusters containing subunit B, and a membrane spanning subunit C, which binds two heme groups. X-ray structure analysis of the complex at 2.2-Å resolution allowed us to identify the electron transfer pathway and to suggest a mechanism for fumarate reduction and succinate dehydrogenation (Lancaster et al. 1999. *Nature*. 402:377).

The yeast cytochrome b_6 -complex could be crystallized with the help of an antibody F_2 -fragment. The structure of the co-complex was determined at 2.3-Å resolution and refined. Many details of the two quinone binding sites (Q_o , Q_i) became known. The structure is compatible with a Q-cycle mechanism of proton transfer ("proton pumping") across the mitochondrial membrane. Five firmly bound lipids were found. Implications of their binding will be discussed.

The cytochrome c oxidase appears to use a completely different mechanism for proton pumping. Electrostatic calculations using the coordinates of the two-subunits-containing enzyme and structural considerations led to the proposal of a novel mechanism (Michel. 1999. *Biochemistry*. 38:15129), which is based on the principle of charge compensation. Each electron transfer into the membrane leads to proton uptake from the opposite side. Some of the protons taken up are electrostatically repelled by protons taken up later and thus pumped. An analysis of published data (Michel. 1999. *Biochemistry*. 38:15129) also led to a revision of those steps of electron transfer, which were supposed to be coupled to proton pumping. The mechanism will be discussed in detail.

8. Atomic Resolution Structures of Bacteriorhodopsin Photocycle Intermediates: The Role of Discrete Water Molecules in the Function of this Light-driven Ion Pump

HARTMUT LUECKE and JANOS K. LANYI, *Department of Molecular Biology & Biochemistry, University of California, Irvine, California 92697-3900*

High-resolution x-ray crystallographic studies of bacteriorhodopsin have tremendously advanced our understanding of this light-driven ion pump during the last 2 yr, and emphasized the crucial role of discrete internal water molecules in the pump cycle. In the extracellular region, an extensive 3-D hydrogen-bonded network of protein residues and seven water molecules leads from the buried retinal Schiff base via water 402 and the initial proton acceptor Asp85 to the membrane surface. Near Lys216, where the retinal binds, transmembrane helix G contains a pi-bulge that causes a nonproline kink. The bulge is stabilized by hydrogen-bonding of the main-chain carbonyl groups of Ala215 and Lys216 with two buried water molecules located in the otherwise very hydrophobic region between the Schiff base and the proton donor Asp96 in the cytoplasmic region. The M intermediate trapped in the D96N mutant corresponds to a late M state in the transport cycle, after protonation of Asp85 and release of a proton to the extracellular membrane surface, but before reprotonation of the deprotonated retinal Schiff base. The M intermediate from the E204Q mutant corresponds to an earlier M; as in this mutant, the Schiff base deprotonates without proton release. The structures of these two M states reveal progressive displacements of the retinal main chain and side chains induced by photoisomerization of the retinal to 13-cis,15-anti, and an extensive rearrangement of the 3-D network of hydrogen-bonded residues and bound water that accounts for the changed pKas of the Schiff base, Asp85, the proton release group, and Asp96. The structure for the M state from E204Q suggests, moreover, that relaxation of the steric conflicts of the distorted 13-cis,15-anti retinal plays a critical role in the reprotonation of the Schiff base by Asp96. Two additional waters now connect Asp96 to the carbonyl of residue 216, in what appears to be the beginning of a hydrogen-bonded chain that would later extend to the retinal Schiff base. Based on the ground state and M intermediate structures, models of the molecular events in the early part of the photocycle are presented, including a novel model that proposes that bacteriorhodopsin pumps hydroxide (OH^-) ions from the extracellular to the cytoplasmic side.

9. F_o Sector of Rotary ATP Synthase: Structure and Mechanism ROBERT H. FILLINGAME, *Department of Biomolecular Chemistry, University of Wisconsin Medical School, Madison, Wisconsin*

ATP is synthesized during oxidative phosphorylation by proton transport-coupled rotary catalysis in the F_1F_o ATP synthase. Proton transport through the transmembrane F_o sector is coupled to rotation of subunit γ within the F_1 sector of the enzyme at the periphery of the membrane. An oligomeric ring of 12 c subunits provides the proton binding sites, which become alternately accessible to channels from the two sides of the membrane as the ring turns in a 12-step fashion. Proton transport occurs at the interface between a single copy of subunit a and the rotating ring of subunit c . In this talk, I will focus on the organization of subunits in the F_o sector of the enzyme and the structural relationship to models of rotary catalysis. A model of the c oligomer has been built based on the NMR structure of monomeric subunit c and cross-linking distance constraints between the two helices of neighboring subunits. The model predicts that transmembrane helices at the periphery of the c -ring must rotate to expose the proton-binding carboxylate of residue cAsp61 to the alter-

nate access channels in subunit *a*. The proposed turning of helices would also explain the cross-linking pattern observed between subunits *a* and *c*. The proton-transport-driven rotation of helices is proposed to drive the stepwise movement of the ϵ -ring and ultimately the turning of the γ subunit within F_1 . (Supported by NIH grant GM23105.)

10. The Kamikaze Approach to Membrane Protein Structure and Function H.R. KABACK, *Howard Hughes Medical Institute, Departments of Physiology and Microbiology & Molecular Genetics, University of California Los Angeles, Los Angeles, California 90095*

Encoded by the *lacY* gene of *E. coli*, the lac permease catalyzes the coupled stoichiometric translocation of a galactoside and a proton. Lac permease has been solubilized from the membrane, purified in a completely active state, and shown to function as a monomer. The protein contains 12 α -helices that traverse the membrane in zigzag fashion connected by relatively hydrophilic loops with both NH_2 and COOH termini on the cytoplasmic face. In a functional permease mutant devoid of native Cys residues, each residue has been replaced with Cys. Analysis of the mutant library has led to the following developments. (a) The great majority of the mutants are expressed normally in the membrane and exhibit significant activity, and only six side chains are clearly irreplaceable for active transport. Glu126 (helix IV), Arg144 (helix V), and possibly Glu269 (helix VIII) are absolutely required for substrate binding, and Arg302 (helix IX), His 322 and Glu325 (helix X) are irreplaceable with respect to proton translocation and/or coupling. (b) Helix packing, tilts, and ligand-induced conformational changes have been determined by using a battery of site-directed biochemical and biophysical techniques. (c) Positions that are accessible to solvent have been revealed. (d) Positions where the reactivity of the Cys replacement is increased or decreased by ligand binding have been identified. (e) The permease has been shown to be a highly flexible molecule. (f) A working model for lactose/proton symport has been formulated.

11. Electron Microscopy and Modeling of P-type Ion Pumps HOWARD S. YOUNG,* WILLIAM J. RICE,* CHEN XU,* JOHN SACHS,† DWIGHT MARTIN,‡ WERNER KÜLBRANDT,§ and DAVID L. STOKES,* *Skirball Institute for Biomolecular Medicine, New York University School of Medicine, New York, New York; †State University of New York, Stony Brook, Stony Brook, New York; and §Max Planck Institute für Biophysik, Frankfurt, Germany

The family of P-type ion pumps are responsible for generating ion gradients across cell membranes in a wide variety of organisms. Such gradients require energy and it is the job of these pumps to couple the hydrolysis of ATP to transport of their respective ions. To understand the structural basis for this energy coupling, we are using electron microscopy to study tubular crystals of both Ca^{2+} -ATPase from rabbit muscle sarcoplasmic reticulum and Na^+/K^+ -ATPase from duck salt glands. In both cases, crystallization requires the addition of vanadate and an absence of the primary transport ion (Ca^{2+} or Na^+), which strongly suggests that the E_2 conformation of the enzyme is present in the crystals. The conformational change between E_2 and E_1 is a key step in coupling ion binding within the membrane to ATP use within the cytoplasmic domain. This involves formation of a transient aspartyl phosphate, by which the pump harnesses the en-

ergy of ATP. In a subsequent step, the pump undergoes a related conformational change, which alters the sidedness of ion binding and dramatically lowers its affinity. We have compared our 3-D structures for the E_2 conformation of Ca^{2+} -ATPase and Na^+/K^+ -ATPase with a structure for H^+ -ATPase from *Neurospora* that we believe corresponds to the E_1 conformation. Dramatic changes in the domain organization of the cytoplasmic head are apparent, whereas the 10 transmembrane helices appear to have a rather similar organization. To interpret these differences, we have modeled the structure of the phosphorylation domain, based on a distantly related bacterial enzyme: L-2 haloacid dehalogenase. This enzyme adopts a Rossman fold with a conserved ligand binding site at the interface between two domains. By fitting the modeled structure for the phosphorylation domain into our 3-D map for Ca^{2+} -ATPase, we propose particular domain movements that account for the very open arrangement of domains in the E_1 conformation. We have considered the specific conformational effects of forming the aspartyl phosphate with reference to the group of bacterial receiver domains, such as CheY. These proteins have a different topology, but the architecture of the active site is the same as the dehalogenase and the effects of phosphorylation have been characterized by x-ray crystallography. According to our proposed structural analogy, phosphorylation would induce a significant movement of the two segments connecting the phosphorylation and nucleotide-binding domains; if amplified by a relatively long lever arm, this movement could account for the dramatic rearrangement observed in the pump cytoplasmic domains. By improving the resolution of our structures, we hope to reveal more subtle changes amongst the transmembrane helices, which would reflect expected changes in ion binding and allow us to speculate about the structural coupling between ion binding and nucleotide binding sites.

12. Structure and Conformational Dynamics of the H^+ -translocating P-type ATPase GENE A. SCARBOROUGH, *Department of Pharmacology, University of North Carolina, Chapel Hill, North Carolina*

Large 3-D crystals of the dodecylmaltoside complex of the *Neurospora* plasma membrane H^+ -ATPase grow under conditions optimized for moderate supersaturation of both the protein and detergent micellar surfaces. Large 2-D H^+ -ATPase crystals also grow at the air-water interface of such crystallization mixtures and on carbon films placed in contact with them. Electron crystallographic analysis of the 2-D crystals has elucidated the structure of the H^+ -ATPase at a resolution of 8 Å in the membrane plane. The 2-D crystals consist of two offset layers of donut-shaped ATPase hexamers with their exocyttoplasmic surfaces face to face. The crystal packing forces appear to comprise both protein-protein and detergent-detergent interactions, supporting the validity of the original crystallization strategy. 10 transmembrane helices in each ATPase monomer are clearly defined in the structure map. The helices are relatively straight, closely packed, moderately tilted at various angles with respect to the membrane normal, and average ~ 35 Å in length. The transmembrane helix region is connected in at least three places to the larger cytoplasmic region, which comprises several discrete domains separated by relatively wide, deep clefts. Several lines of biochemical evidence indicate that the H^+ -ATPase undergoes substantial conformational changes during its catalytic cycle that are not changes in secondary structure. And, importantly, the results of hydrogen/deuterium exchange experiments indicate that these conformational changes are most likely rigid body in-

terdomain movements that lead to cleft closure. When interpreted within the framework of established principles of enzyme catalysis, this information on the structure and dynamics of the H⁺-ATPase molecule provides the basis of a rational model for the sequence of events that occur as the ATPase proceeds through its transport cycle. The forces that drive the sequence can also be clearly stipulated, and stem from transition state binding energy. Insights as to the molecular mechanism by which these conformational dynamics energize concentrative proton translocation will hopefully emerge when an atomic structure of a P-type ATPase is obtained. (Supported by NIH grant GM-24784.)

13. Action of Agonists and Antagonists on the AMPA GluR2 Receptor Ligand Binding Core ERIC GOUAUX, NEALI ARMSTRONG, and RONGSHENG JIN, *Department of Biochemistry and Molecular Biophysics, Columbia University, New York, New York*

Ionotropic glutamate receptors (iGluRs) define a family of ligand-gated ion channels that are essential for the development and function of the mammalian nervous system and are implicated in processes that include memory and learning, and diseases such as schizophrenia. Within the iGluR family of receptors, pharmacologically distinct subtypes include the AMPA, kainate, and NMDA receptors. The region of iGluRs that defines receptor pharmacology is the ligand-binding core or S1S2 region. My laboratory has developed methods for the over-expression and folding of the GluR2 (AMPA) S1S2, and has crystallized it alone and with a series of ligands. Here I report the structures of the bilobed GluR2 S1S2 core in an apo form and bound to the agonists AMPA, glutamate, and kainate, and the antagonist DNQX. Agonists and antagonists bind between domains 1 and 2, bring the domains closer together, and reduce the volume of the interdomain cleft. By contrast, in the apo and the antagonist-bound state, the domains are significantly farther apart and the active site cleft is expanded. Partial agonists such as kainate produce a degree of domain separation that is intermediate between the glutamate- or AMPA-bound state and the apo form. Recent high resolution studies involving a series of five-substituted Wilardiine compounds (H, F, Br, and I) will also be discussed.

14. Structural Underpinnings of Voltage Sensing in Potassium Channels F. BEZANILLA, D. STARACE, A. CHA, and P.R. SELVIN, *Departments of Physiology and Anesthesiology, University of California, Los Angeles, School of Medicine, Los Angeles, California; and Department of Physics, University of Illinois at Urbana-Champaign, Urbana, Illinois*

The steep voltage dependence of the open probability in voltage-dependent channels is the result of moving ~12 electronic charges in the membrane field. This charge movement is the gating current that gives an electrical indication of the conformational changes of the voltage sensor. We have investigated the molecular basis of this charge movement in sodium and potassium channels using histidine-scanning mutagenesis and site-directed fluorescence labeling. The rationale of histidine scanning is that this amino acid may substitute the basic residues of the voltage sensor and it can be titrated in a pH range that can be tolerated by the biological preparation, allowing the study of proton accessibility. Our results indicate that the first four charged residues of the S4 segment of *Shaker* K channel change accessibility from the inside at hyperpolarized potentials to outside at depolarized po-

tentials. These results combined with reports on cysteine-scanning mutagenesis indicate that these four charges reside in long crevices with ends too narrow to fit MTS reagents, but large enough to allow protons to access them. We have labeled specific sites in the S1-S2 linker, the S3-S4 linker, and the S4 segment with fluorescent probes that undergo changes in quenching as a result of membrane potential changes. These changes indicate local conformational changes during the reorientation of the voltage sensor. To quantify these changes, we used lanthanide-based resonance energy transfer (LRET) measurements on equivalent residues between subunits. The results support the idea that the S4 segment undergoes a rotation with little or no translation when the membrane potential changes. The combined results of histidine-scanning mutagenesis and LRET suggest a model for the S4 operation whereby the charges that are in an internally exposed crevice at hyperpolarized potentials rotate to become exposed into an externally connected crevice upon depolarization.

15. A Structural Perspective of Activation Gating in K⁺ Channels EDUARDO PEROZO, YI-SHIUAN LIU, PORNTHEP SOMPORNPISUT, MARIEN CORTES, and LUIS G. CUELLO, *Department of Molecular Physiology and Biological Physics, University of Virginia, Charlottesville, Virginia*

In the *Streptomyces* K⁺ channel (KcsA), a concerted rotation and translation of the two transmembrane segments leads to channel opening in a pH-dependent manner (Cuello et al., *Biochemistry*. 37:3229, Perozo et al., *Science*. 285:73). These movements are reversible and occur in a pH-dependent manner. To further understand the mechanisms underlying pH-dependent gating in KcsA, both functional and structural information of the channel cytoplasmic domains are required. To generate more precise models of these helix movements in KcsA, inter- and intrasubunit distances are required. Yet, a quantitative assessment of spin-spin dipolar couplings in oligomers of $n > 2$ is usually hampered by the presence of multiple potential labeling sites. One strategy to facilitate single distance determinations in spin-labeled KcsA is to construct tandem dimer channels in which only one of the linked elements can be spin labeled. Under these conditions, spin-spin coupling can occur only among diagonally related subunits. Residues with strong spin-spin coupling located on TM2 and the COOH-terminal end of the channel were selected to compare structural differences between tandem dimers and KcsA. Intersubunit distances have been determined for selected residues in the closed and open conformations of the channel. Data on probe mobility (ΔH_{O}^{-1}), O₂ and NiEdda accessibility parameters (Π_{O_2} and Π_{NiEdda}), and spin-spin interaction (Ω) were used as structural constraints for a set of algorithms based on Distance Geometry methods, Simulated Annealing and Restrained Molecular Dynamics. Results from these calculations are interpreted in terms of changes in interhelix angles and translations. The current gating models for KcsA will be discussed in light of these results. (Supported by NIH grants GM54690 and GM57846 and The McKnight Endowment Fund.)

16. Physical Location of T1 Domain in the *Shaker* Potassium Channel OLGA SOKOLOVA and NIKOLAUS GRIGORIEFF, *W.M. Keck Institute for Cellular Visualization, Rosenstiel Basic Medical Sciences Research Center, Brandeis University, Waltham, Massachusetts* (Sponsor: Christopher Miller)

We have determined the physical location of the T1 domain within the *Shaker* potassium channel using electron microscopy. Images of single, detergent-solubilized channels in negative stain were analyzed on a computer using single particle averaging techniques. Depending on their orientation, some channels display a clear fourfold symmetry (Li et al. 1994. *Curr. Biol.* 4:110) corresponding to the tetrameric structure of *Shaker*. Other channels are visible from the side with the pore axis parallel to the image plane. In the side views, the T1 domains can be distinguished as separate densities ~ 10 Å away from the membrane domains of the channel. The T1 domains are connected to the membrane domains by weaker density, leaving ~ 10 -Å holes between the domains. The data supports a "hanging basket" model for the T1 domain where the NH_2 -terminal inactivation domain gains access to the pore through the holes.

17. Mechanism of Ion Conduction and Selectivity in K Channels RODERICK MACKINNON, *Laboratory of Molecu-*

lar Neurobiology and Biophysics, Howard Hughes Medical Institute and The Rockefeller University, New York, New York 10021

Potassium channels are proteins that control the passive flow of K^+ ions across cell membranes. This K^+ flow is necessary for producing electrical signals in the nervous system, for governing the rate at which our hearts beat, and for the secretion of specific hormones such as insulin. There are many different kinds of K^+ channels, but they are all built on a common theme; all have four identical subunits surrounding a central membrane-spanning pore. The pore is ion selective, ensuring that only K^+ (radius 1.33 Å) and not Na^+ (radius 0.95 Å) enters and crosses the cell membrane. The structure of the *Streptomyces lividans* K^+ channel revealed an elegant mechanism by which the dielectric barrier, the fundamental electrostatic impediment to transmembrane ion flow, is lowered by a water-filled cavity and precisely oriented alpha helices. The structure also shows how the pore holds a queue of three K^+ ions. Two of the ions are nearly completely dehydrated in a region called the selectivity filter. In this region, where K^+ versus Na^+ discrimination takes place, oxygen atoms from the protein have replaced the water.

POSTER ABSTRACTS

18. How Many Anion Binding Sites Are There in the CFTR Channel Pore? ZHEN ZHOU and TZYH-CHANG HWANG, *Department of Physiology, Dalton Cardiovascular Research Center, University of Missouri-Columbia, Columbia, Missouri*

It is controversial whether the CFTR chloride channel contains a multi-ion pore. We used channel blockers to explore the anion binding site(s) in the CFTR channel pore. K1250A-CFTR, a mutant CFTR that can stay open for minutes once opened, permits kinetic analysis of the blocking events in isolation of gating transitions. Within the prolonged opening, there are numerous brief closings that are referred to as fast flickers, as seen in wild-type CFTR channels. These intrinsic flickers, likely caused by transient block of the channel from the cytoplasmic side of the membrane, have been shown to be voltage dependent. Surprisingly, our results show that the off rate, but not the on rate, is voltage dependent, and this voltage dependence of off rates can be abolished by removing external permeant anions, suggesting that the binding site of the intrinsic blocker is not deep in the pore. Instead of sensing the transmembrane voltage by the blocker itself, the blocker acquires the voltage-dependent off rate through electrostatic interaction with a neighboring Cl^- in the pore. These observations are consistent with a mechanism that can place the unknown blocker and permeant chloride ions in the aqueous pore simultaneously. It is likely that the binding site of the intrinsic blocker is also a Cl^- binding site, since the number of flickers decreased dramatically when millimolar SCN^- was applied to the cytoplasmic side of the channel, suggesting that SCN^- , a Cl^- surrogate, and the intrinsic blocker may compete for a common binding site. Glibenclamide, a known CFTR blocker, was used to further explore the channel pore. Both off and on rates of glibenclamide block are voltage dependent ($\delta = \sim 0.32$ and ~ 0.20 , respectively). Removal of external Cl^- decreased the off rate, suggesting that internally applied glibenclamide and a Cl^- ion from the external entrance can simultaneously occupy the pore. However, the off rate of glibenclamide remained voltage dependent in the absence of external permeant anions ($\delta = \sim 0.19$), suggesting that the glibenclamide binding site, unlike that for the intrinsic blocker, resides deeper in the channel pore. Our results can be explained by a model that places at least three anion binding sites in the CFTR pore (from cytoplasmic end to extracellular end): a superficial site where the intrinsic blocker binds, a deep site for glibenclamide, and a more external site, Cl^- occupancy of which affects glibenclamide binding.

19. Folding Determinants for Gramicidin Channels in Membranes DENISE V. GREATHOUSE,* S. SHOBANA,† ROGER E. KOEPPE II,* and OLAF S. ANDERSEN,‡ *Department of Chemistry and Biochemistry, University of Arkansas, Fayetteville, Arkansas 72701; and †Weill Medical College of Cornell University, New York, New York 10021

Aromatic side chains, especially the indole of Trp and the phenol of Tyr, play special roles in transmembrane proteins and tend to cluster at the membrane/water interface (Michel and Deisenhofer. 1990. *Curr. Top. Membr. Transp.* 36:53–69; Cowan et al. 1992. *Nature.* 358:727–733; Landolt-Marticorena et al. 1993. *J. Mol. Biol.* 229:602–608; Doyle et al. 1998. *Science.* 280:69–77). In gramicidin channels, the four tryptophans near the COOH terminal of each subunit dictate the conformation of a functional membrane-spanning dimer, including the helix winding (“strandedness”) and helix sense (“handedness”) of the channel-forming $\beta^{6,3}$ conformation. The importance of the Trp residues is shown also by the fact that when the native (Trp-D-Leu)₃Trp sequence is modified to (Leu-D-Trp)₃Leu, not only do the preferred strandedness and handedness vary, but a single chemical species assumes three different interconverting channel conformations. The functional signatures of these three conformers allow their relative folding energetics to be determined. These single-channel characterizations are confirmed and complemented by circular dichroism and magnetic resonance spectroscopic studies, and by molecular dynamics simulations. The “simple” gramicidin channel has a folding complexity that is closely coupled to its detailed amino acid sequence. (Supported by NIH grants GM-34968 and GM-21342.)

20. Voltage-dependent Gating of a Homodimeric Gramicidin Channel with a Chiral Mismatch ROGER E. KOEPPE II,* SIGRID E. SCHMUTZER,* ERIC MILLER,* GWENDOLYN L. MATTICE,* DENISE V. GREATHOUSE,* LYNDON L. PROVIDENCE,† and OLAF S. ANDERSEN,‡ *Department of Chemistry and Biochemistry, University of Arkansas, Fayetteville, Arkansas 72701; and †Weill Medical College of Cornell University, New York, New York 10021

Gramicidin channels are composed of two subunits that are joined, in the middle of the bilayer, by six hydrogen bonds at their formyl-NH-termini. Gramicidin channels usually are not

voltage dependent. Nevertheless, some symmetry-breaking dipolar side-chain substitutions in gramicidin A (gA) introduce voltage dependence if present near the bilayer center in only one of the subunits. For example, $[F_6Val^1]gA/[Val^1]gA$ heterodimeric channels exhibit voltage-dependent transitions between two conducting states (Oiki et al. 1995. *Proc. Natl. Acad. Sci. USA*. 92: 2121–2125). The distribution between the low- and high-conducting states varies as a function of the applied potential, but is not dependent on whether the permeant ion is H^+ or Cs^+ . The property of voltage-dependent gating is restricted to a small subset of all known modified gramicidin channels and, until now, has been observed only in heterodimeric examples. Recently, we synthesized a new gramicidin and discovered that even the homodimeric channels have a bi-stable conductance and exhibit voltage-dependent gating. The new gramicidin is (des-Val¹)-[Ala²]gA, which has the sequence formyl-AA $\underline{L}A^5$ $\underline{V}V$ $\underline{V}W^9$ $\underline{L}W^{11}$ $\underline{L}W^{13}$ $\underline{L}W^{15}$ -ethanolamine, in which amino acids of D-chirality are underlined. Des-Val¹-[Ala²]gA is shortened to 14 residues and begins with L-alanyl-L-alanine instead of a strictly alternating (L,D) sequence. (Although Val¹ has been deleted, we begin the numbering with Ala² to retain consistency with the conventional numbering system for gA.) What is the chemical origin of the gating behavior, and why is the phenotypic signature of the homodimeric (des-Val¹)-[Ala²]gA/(des-Val¹)-[Ala²]gA channels qualitatively similar to that of the heterodimeric $[F_6Val^1]gA/[Val^1]gA$ channels? These questions are the subject of ongoing investigations, but a plausible and consistent hypothesis would be that the gating transitions in either system may be attributed to a stress on the peptide backbone at the subunit junction and near the bilayer center. In one case, the stress would be induced by the asymmetric F_6Val residue (because of the larger bulk of a CF_3 as compared with a CH_3); in the other case, the stress would be induced by the Ala² of the wrong chirality (L-Ala² where D-Ala² is expected). Importantly, the existence of gated (or just bi-stable) gramicidin homodimers opens new possibilities for mechanistic studies using spectroscopic methods; for example, solid-state deuterium magnetic resonance experiments using oriented samples. (Supported by NSF grant MCB-9816063 and NIH grant GM21342.)

21. Kinetic Studies on Ion Movement through a Channel of Known Structure OLAF S. ANDERSEN,* MURRAY D. BECKER,* DENISE V. GREATHOUSE,† and ROGER E. KOEPE II,‡ *Weill Medical College of Cornell University, New York, New York 10021; and †Department of Chemistry and Biochemistry, University of Arkansas, Fayetteville, Arkansas 72701

The gramicidin channels constitute a family of membrane-spanning, ion-permeable channels of known structure and well-defined function. Gramicidin channels are selective for small monovalent cations, and the channels' permeability characteristics can be studied over a wide range of permeant ion concentrations and membrane potential differences. The gramicidin channels thus become useful for examining the mechanism(s) of ion permeation through membrane-spanning channels. It is possible to define a minimal kinetic model, based on a discrete-state scheme, that accounts for the channels' ion permeability. The magnitude of the rate constant for passage through the pore, from one "binding site" to the other, is consistent with an electrodiffusive transfer over a barrier of a few kT. The changes in the association and dissociation rate constants for the double-occupied relative to the single-occupied states cannot be reconciled

within a simple electrostatic repulsion model. The most likely explanation is that one needs to consider also the water movements associated with ion entry and exit. This model is used to analyze the mechanisms by which changes in the channel-forming gramicidins' amino acid sequence can alter the rate of Na^+ movement through the channel. Results on gramicidin channels with single Trp→Phe substitutions (one in each channel-forming monomer) show that the substitutions alter all rate constants in the kinetic scheme, with differential effects on single- and double-ion occupied states. (Supported by NIH grants GM21342 and GM34968.)

22. Mechanical Properties of Biological Membranes: Gramicidin Channels as Molecular Force Transducers CLAUS NIELSEN,* OLAF S. ANDERSEN,† DENISE V. GREATHOUSE,‡ and ROGER E. KOEPE II,§ *August Krogh Institute, University of Copenhagen, DK-2100 Copenhagen Ø, Denmark; †Weill Medical College of Cornell University, New York, New York 10021; and ‡Department of Chemistry and Biochemistry, University of Arkansas, Fayetteville, Arkansas 72701

Changes in membrane lipid composition alter membrane protein function, but the relations between membrane protein function and the chemical and physical properties of the host lipid bilayer have long been elusive. Traditionally, membrane-protein interactions have been described in terms of changes in membrane fluidity, but a change in bilayer fluidity alone cannot explain a shift in the conformational preference of integral membrane proteins. Structural studies on membrane proteins show that membrane protein function may involve changes in protein structure that affect the protein-lipid boundary. The hydrophobic coupling between a protein's membrane-spanning domain and the bilayer core thus will cause a protein conformational change to perturb the surrounding bilayer. Conversely, the bilayer will impose energetic constraints on the conformational preference of membrane proteins. Gramicidin channels can be used as molecular force transducers to quantify the energetic cost of the bilayer deformation associated with membrane protein conformational change. The formation of head-to-head dimers with the Trp residues anchoring each monomer at the membrane/solution interface constitutes a well defined (albeit unique) conformational change in a membrane protein that allows for examination of the membrane protein interactions as an energetic problem (Andersen et al. 1999. *Methods Enzymol.* 299: 208). We have extended this approach to biological membranes and incorporate different gramicidin analogs (gramicidin channels of different hydrophobic length) in Sf9 cell plasma membranes and use the gramicidin analogues as molecular force transducers to assess the mechanical properties of the membrane in vivo. The experimental results are interpreted using an elastic (liquid crystalline) membrane model that describes the energetics of protein-lipid interactions (Nielsen et al. 1998. *Biophys. J.* 74:1966). (Supported by the Carlsberg Foundation 980106/20-1249 and NIH grants GM21342 and GM34968.)

23. Chemical Modifications in the Gramicidin Channel Backbone SIGRID E. SCHMUTZER,* S. SHOBANA,† LYNDON L. PROVIDENCE,‡ DENISE V. GREATHOUSE,* OLAF S. ANDERSEN,† and ROGER E. KOEPE II,* *Department of Chemistry and Biochemistry, University of

Arkansas, Fayetteville, Arkansas 72701; [†]Weill Medical College of Cornell University, New York, New York 10021

The pore of gramicidin channels as well as the selectivity filter of KcsA potassium channel (Doyle et al. 1998. *Science*. 280:69–77) are lined by peptide backbone carbonyl groups. We are using organic synthesis to replace the amide bond between formyl-Val¹ and Gly² of gramicidin A with other functional groups, including ester and keto-methylene. The ester substitution removes a stabilizing NH · · O = C hydrogen bond and replaces it with a repulsive O · · O = C interaction. The resulting perturbations in the backbone structure and dynamics cause a >1,000-fold reduction in dimer stability and channel lifetime. In addition, the single-channel conductance is reduced by ~10-fold and the Na⁺/Cs⁺ selectivity is inverted, as compared with the native gramicidin A channel. When only one peptide bond is replaced by an ester bond, which leads to an asymmetric heterodimeric channel, the destabilization is less pronounced and the channels exhibit multi-state conductance behavior. Molecular dynamics simulations on the different structures show that the backbone mutations have rather modest effects on the overall channel structure, and identify the local perturbations induced by the substitutions. The findings emphasize the importance of the backbone for ion transport through gramicidin channels and larger channels. To examine this further, we are replacing the NH with CH. This modification also removes the hydrogen bond, but the new interactions should be less repulsive. (Supported by NIH grants GM-34968 and GM-21342.)

24. Hydrogen Bonding Ability of Aromatic Residues Is Important for the Organization of Membrane-Spanning Structures S. SHOBANA,* DENISE V. GREATHOUSE,[†] ROGER E. KOEPPE II,[†] and OLAF S. ANDERSEN,* *Weill Medical College of Cornell University, New York, New York 10021; and [†]Department of Chemistry and Biochemistry, University of Arkansas, Fayetteville, Arkansas 72701*

To determine whether the ability of aromatic residues to form hydrogen bonds with the polar groups at the membrane/solution interface could be important for the conformational preference of membrane-spanning gramicidin channels, we made use of the fact that some combinations of gramicidin analogs allow for the formation of conducting, double-stranded (DS) heterodimeric channels (Durkin et al. 1992. *Biophys. J.* 62:145–159). Specifically, the gramicidin analogs M (gM), gramicidin N (gN), and gramicidin T (gT), in which the four tryptophans in gramicidin A (gA) are replaced by phenylalanine, naphthylalanine, and tyrosine, respectively, by themselves form right-handed, single-stranded (SS) β6.3-helical channels. The sequence-shortened enantiomer des-D-Val1-gA- forms left-handed SS β6.3-helical channels. None of the right-handed β6.3-helical monomers can form heterodimers with a left-handed β6.3-helical monomer, but they can, in principle, form DS channels. The gramicidin analogues gA, gT, gM, and gN were used along with des-D-Val1-gA- to examine the formation of conducting DS hybrid channels. DS hybrid channels were observed frequently with gN/des-D-Val1-gA- and g/des-D-Val1-gA-, but only rarely, if at all, with gT/des-D-Val1-gA- or gA/des-D-Val1-gA-. These results show that the preference for hydrogen bond formation by the tryptophan NH or the tyrosine OH with polar groups at the membrane/solution interface favors the formation of SS channels (or, more properly, hinders the formation of conducting DS heterodimeric channels). Because the naphthylalanines of gN and phenylalanines of gM cannot form hydrogen bonds with polar groups at the mem-

brane/solution interface, there is less penalty for burying these aromatic residues, which means that the formation of conducting DS hybrid channels becomes more favorable. (Supported by a Norman and Rosita Winston Fellowship and NIH grants GM21342 and GM34968.)

25. Structure/Function Studies of Chlamydial Porins ELIZABETH S. HUGHES, KATE M. SHAW, and RICHARD H. ASHLEY, *Department of Biomedical Sciences, University of Edinburgh, Edinburgh, United Kingdom* (Sponsor: David N. Sheppard)

Chlamydial diseases are important threats to animal and human health. The intracellular pathogens share certain structural similarities with gram negative bacteria, including the presence of major outer membrane proteins (MOMPs). MOMPs are highly immunogenic, and leading targets for vaccine development. However, MOMP structures are poorly understood, and uncertainty about the identity of surface-exposed domains limits the engineering of recombinant vaccines. To improve our understanding of MOMP structures, and develop a functional assay for refolded proteins, we purified *C. psittaci* MOMP, confirmed it is a β-sheet rich porin-like ion channel (Wyllie et al. 1998. *Infect. Immunol.* 66:5202–5207), and cloned, expressed, and functionally reconstituted truncated versions of *C. psittaci* and *C. pneumoniae* MOMPs (Wyllie et al. 1999. *FEBS Lett.* 445:192–196). The high-conductance, mildly cation-selective channels have statistically distinct properties, and we are currently carrying out structure/function studies alongside protein crystallization, intending to use functional mapping to help solve MOMP structures by molecular replacement. In this study, we cloned and expressed a full-length *C. trachomatis* MOMP, and investigated the structural role of the “VS4” domain, one of four regions of variable sequence hypothesized to contain one or more surface-exposed loops. Chimaeric channels in which the 33-residue VS4 region of *C. trachomatis* was replaced by that of *C. psittaci* retained the conductance of the original protein, but their selectivity was indistinguishable from that of the full-length *C. psittaci* protein. We next tested the idea that we had transplanted a so-called “pore-confined” loop by expressing and reconstituting a *C. trachomatis* porin lacking its VS4 domain. We obtained functional channels, suggesting that the deleted VS4 contained at least one surface turn or loop and an (even) number of complete β strands. These channels were even more cation selective, and their conductance was similar or reduced. Therefore, it is likely that the pore of the β barrel is partially occluded by a pore-confined loop contributed by another variable domain. (Supported by the Wellcome Trust.)

26. On the Nature and Location of the pH Sensor in the *Streptomyces* K⁺ Channel LUIS G. CUELLO and EDUARDO PEROZO, *Department of Molecular Physiology and Biological Physics, University of Virginia, Charlottesville, Virginia*

The potassium channel from *Streptomyces lividans* KcsA exhibits a characteristic increase in channel activity at acidic pH (Cuello et al. 1998. *Biochemistry*. 10:3229). Recent studies have shown that this pH activation can be observed only by pH changes in the intracellular face of the channel (Heginbotham et al. 1999. *J. Gen. Physiol.* 114:551). Here we report on deletion analysis and site-directed mutagenesis experiments aimed at identifying and char-

acterizing the structural components of this pH sensor. Mutants and deletion constructs were functionally analyzed by their ability to catalyze a Ba^{2+} -blockable, pH-dependent ^{86}Rb uptake. The effects of the mutations on channel stability were studied by a temperature-dependent gel-shift assay.

We found small effects on the pH dependence and activation pKa for COOH-terminal truncations up to residue F125 from deletion experiments. Truncations around residue T141 and beyond produced virtually no effects. These results suggest that any structure responsible for pH dependency is probably located at or very close to the transmembrane segments of the channel. Thus, we concentrated on a cluster of charged residues adjacent to the narrowest part of the conducting pathway of the channel containing six putative charged groups. Residues R117, E118, R120, R121, R122, and H124 were mutated to cysteine, and their pH dependency was evaluated using rubidium influx experiments. All residues showed some reduction in pH dependency, with the exception of H124. The largest changes were observed at positions 117, 118, and 120. A more detailed characterization of the role of these amino acids is being explored using cysteine modification with charged MTS reagents in addition to additional combinatorial neutralizations of each of the charged residues to glutamine. Preliminary results suggest that pH dependence in KcsA cannot be attributed to a single charged residue. (Supported by NIH grants GM54690 and GM57846, and The McKnight Endowment Fund.)

27. Towards Design and Synthesis of a Specific and High-Affinity Blocker of Cyclic Nucleotide-gated Channels AMBARISH S. GHATPANDE, VERNON Y. YOST, and JEFFREY W. KARPEN, *Department of Physiology and Biophysics, University of Colorado Health Sciences Center, Denver, Colorado*

Cyclic nucleotide-gated (CNG), cation-selective channels generate electrical responses to light and odors in the visual and olfactory systems. CNG channels are found in the brain and in a variety of other tissues where their roles are less well defined. A major handicap in elucidating the roles played by CNG channels is the lack of specific, high-affinity toxins or blockers. To address this problem, we designed a specific and high-affinity blocker using the polymer-linked ligand dimer (PLD) approach described recently (Kramer and Karpen. 1998. *Nature*. 395:710–713). In general, for a protein having two or more ligand binding sites, a major enhancement ($\sim 1,000$ -fold) over intrinsic ligand affinity can be obtained if the ligands are linked together with an appropriate length polymer. We chose cyclic GMP, with four binding sites on the channel, and tetracaine, a high-affinity but nonspecific pore blocker (Schnetkamp. 1987. *Biochemistry*. 26:3249–3253), as the two ligands, with polyethylene glycol (PEG) serving as a flexible and variable-length linker. In essence, the affinity enhancement afforded by the cyclic GMP moiety makes the PLD specific for CNG channels. We synthesized various tetracaine derivatives to find an appropriate place to attach PEG without abolishing block. Blocking characteristics of these derivatives will be discussed. The most potent tetracaine derivative synthesized to date had a K_i of 80 nM for the homotetrameric rod CNG channel. We were able to attach a PEG (3,400 D) to this compound without excessive loss in affinity ($K_i \sim 20 \mu\text{M}$). Blocking characteristics of this compound coupled to cyclic GMP and the implications for developing specific, high-affinity blockers using the PLD approach will be discussed. (Supported by NIH grant EY-09275.)

28. Conformational Changes in the S6 Regions of Rod Cyclic Nucleotide-gated Channels GALEN E. FLYNN and WILLIAM N. ZAGOTTA, *Department of Physiology and Biophysics, Howard Hughes Medical Institute, University of Washington, Seattle, Washington*

Rod cyclic nucleotide-gated channels (CNG1) are activated by the direct binding of cGMP to an intracellular domain in the carboxyl-terminal region. The binding of ligand initiates a sequence of molecular events that results in the opening of the channel pore. We asked the question: does the S6 region, which is predicted to line the inner vestibule of these channels, undergo conformational changes associated with gating? Guided by the structure of KcsA channels, we constructed a homology model of the CNG1 channel S5-pore-S6 regions. This model was used to make testable predictions of amino acid accessibility and side chain orientation. To test our predictions, we introduced cysteines into 12 sites in the S6 region of a cysteine-free alpha subunit of the rod CNG channel (CNG1c7). Consistent with our homology model, which predicts the cytoplasmic ends of the S6 helices are in close proximity to each other, we found spontaneous disulfide bonds form between S399C residues in neighboring subunits. Interestingly, these disulfide bonds only form when S399C channels are in the closed state and not when they are in the open state. We also measured the rate of modification by MTS reagents of a number of cysteines introduced in the S6 helices. We have determined the modification rates of T360C, V384C, V391C, and S399C by MTSEA and found them to be similar for both open and closed states of these channels. Our results suggest that the S6 region of CNG1 channels undergoes a conformational change associated with gating and the activation gate is within or beyond the selectivity filter in the permeation pathway.

29. A Point Mutation in the S2–S3 Loop of the Olfactory Cyclic Nucleotide-gated Ion Channel Alters Its Sensitivity to Agonists, Voltage, and Inhibitors JENNIFER I. CRARY, DYLAN M. DEAN, WANG NGUITRAGOOL, and ANITA L. ZIMMERMAN, *Department of Molecular Pharmacology, Physiology and Biotechnology, Brown University, Providence, Rhode Island*

Cyclic nucleotide-gated (CNG) ion channels are nonselective cation channels that open in response to cyclic nucleotides. In the visual and olfactory systems, the CNG channels are essential components of the sensory transduction pathways. The rod and olfactory CNG channels have been cloned and are well characterized by electrophysiological techniques after expression in heterologous systems such as *Xenopus* oocytes. The alpha homomultimers of the two channels have been shown to have different sensitivities to the agonists, cGMP and cAMP, as well as to the inhibitor, tetracaine. We have recently shown that the two channels are also differentially inhibited by diacylglycerol. Using chimeras, others have identified several regions throughout the channel structure that contribute to the differences in gating (Gordon and Zagotta. 1995. *Neuron*. 14:857–864; Goulding et al. 1994. *Nature*. 372:369–374). Here, we examine a rat olfactory mutant, Rolf G204W, which contains a single residue mutation in the S2–S3 loop, but behaves more like the rod channel than its wild type counterpart. It demonstrates reduced sensitivity to cyclic nucleotides (cAMP is only a partial agonist) and increased sensitivity to tetracaine and diacylglycerol. In addition, like the rod channel, Rolf G204W demonstrates a weak voltage dependence with prominent gating kinetics not seen in records from the wild-type rat olfactory channel. (Supported by NIH R01 EY07774 and RI AHA 97-07721S.)

30. Functional Analysis of Recombinant SK Channels YING-JUN CAO,* BABAK S. JAHROMI,† MICHAEL T. ROBERTS,* JESSICA L. RICHARDSON,* JOHN C. DREIXLER,* and KHALED M. HOUAMED,* *Department of Anesthesia and Critical Care, and †Department of Neurobiology, Pharmacology and Physiology, The University of Chicago, Chicago, Illinois

SK channels are small-conductance, calcium-activated potassium channels distinguished by exquisite sensitivity to intracellular calcium and by voltage-independent gating. Neuronal SK channels underlie slow afterhyperpolarization and mediate spike frequency adaptation. Non-neuronal SK channels appear to be involved in regulating cellular proliferation. Recent cloning and expression studies have revealed multiple SK channels encoded by a gene family distantly related to *Shaker*. This family is conserved from mammals to nematodes and flies. Mammalian SK channels appear to be structurally similar to *Shaker*, having six putative transmembrane domains and a pore loop. SK channels share a common calcium-sensing mechanism. This is done by means of a calmodulin molecule tightly associated with the carboxyl terminus of each SK channel subunit. We have characterized subtype-dependent differences in functional properties of recombinant SK channels. We have found that unitary conductance varies approximately twofold between different recombinant SK channels. Different SK channel subtypes also differ in their calcium-dependent gating, with the maximal opening probability differing approximately fourfold. Recombinant SK channels inwardly rectify. They also differ in pharmacological responses to blockers and openers. The biophysical mechanisms underlying these properties are currently under study.

31. Structural Locus for Cation Regulation of ROMK H. SACKIN,* S. SYN,* H. CHOE,† L.G. PALMER,* and E. WALTERS,* *The Chicago Medical School, North Chicago, Illinois; and †Weill Medical College of Cornell University, New York, New York

The effect of external potassium (K) and cesium (Cs) on the inwardly rectifying K channel, ROMK2 ($K_{ir}1.1b$), was studied in *Xenopus* oocytes. Elevating external K from 1 to 10 mM progressively increased whole-cell outward conductance by a factor of 3.4 ± 0.4 in 15 min and by a factor of 5.7 ± 0.9 in 30 min ($n = 22$). Replacing external Na by Cs blocked inward conductance but increased whole-cell conductance by a factor of 4.5 ± 0.5 over a period of 40 min ($n = 15$). This type of time-dependent channel activation was not seen with IRK1. Replacing any one of four ROMK2 residues: F129, K61, L117, or V121 by their respective IRK1 homologues abolished the slow increase in ROMK whole-cell conductance, although a small, rapid increase in conductance still occurred as soon as high K or Cs came in contact with the membrane. The slow increase in conductance is interpreted as activation of pre-existing ROMK channels that had been inactivated by low external K. These results are consistent with a model in which ROMK can exist in either an active mode or a collapsed (inactive) mode. Within the active mode, individual channels undergo rapid transitions between open and closed states. High (10 mM) external K or Cs stabilizes the active mode, and low internal pH stabilizes the inactive mode. Any one of the three ROMK2 point mutations, F129C, L117I, or V121T, prevents external cation-dependent activation, whereas the mutation K61M blocks inactivation by internal protons. One interpretation of these observations is that a residue at the outer mouth

of the pore (F129) or residues within the permeation path (near L117 or V121) function as "K sensors" for extracellular K.

32. The COOH-Terminal Tails of Sulfonyl Urea Receptors Control ADP-dependent Activation of ATP-sensitive K^+ Channels and Their Modulation by Diazoxide KENJI MATSUSHITA,* TETSURO MATSUOKA,* YUSUKE KATAYAMA,* AKIKAZU FUJITA,* YOSHIHISA KURACHI,* and HARUKI NAKMURA,† *Department of Pharmacology II, Graduate School of Medicine, and †Protein Institute, Osaka University Suita, Osaka, Japan

The ATP-sensitive K^+ (KATP) channels are composed of Kir6.0 subunits and sulfonyl urea receptors (SUR1, SUR2A, and SUR2B). SUR1, SUR2A, and SUR2B are characteristic for the pancreatic, cardiac, and smooth-muscle-type KATP channels, respectively. Roles of structural elements of SURs have not been fully clarified. Here we report that the 42 amino acid segment at the COOH-terminal tail of SURs plays a critical role in differential activation of various KATP channels by ADP and its modulation by diazoxide. In the inside-out patches of the HEK293T cells coexpressing distinct SURs and Kir6.2, we examined activation of KATP channels by ADP and diazoxide. We found that, in the presence of 1 mM ATP, much higher concentrations of ADP were needed to activate SUR2A/Kir6.2 channel than SUR1 or SUR2B/Kir6.2. In all SUR/Kir6.2 channels, diazoxide increased the potency of ADP for channel activity without affecting its efficacy. The replacement of the 42 amino acid COOH-terminal tail of SUR1 to that of SUR2A (chimera SUR1-2A) greatly attenuated the ADP-mediated activation of the KATP channel and its modulation by diazoxide. The point mutations of the second nucleotide binding domain (NBD2) of SUR1 and SUR2B, which are known to inhibit ADP-binding, showed similar effects to the chimera and SUR2A. Therefore, it is suggested that the COOH-terminal tail of SUR2A suppresses the ADP-binding to NBD2 of SURs, and thus high concentrations of ADP were required for diazoxide-mediated activation of the SUR2A/Kir6.2 channel.

33. Tetrameric T1 Domain in a Functioning *Shaker* K^+ Channel WILLIAM R. KOBERTZ and CHRISTOPHER MILLER, Howard Hughes Medical Institute, Department of Biochemistry, Brandeis University, Waltham, Massachusetts

The T1 domain of voltage-gated K^+ channels is a highly conserved cytoplasmic region (~120 amino acids) located NH₂ terminal to the first membrane-spanning sequence. Crystal structures of several isolated T1 domains have been solved (Kreusch et al. 1998. *Nature*. 392:945-948; Bixby et al. 1999. *Nat. Struct. Biol.* 6:38-43). These structures are fourfold tetramers ($40 \times 40 \times 20$ Å) with the tetramerization interface composed primarily of hydrogen bonds. Symmetry requires the T1 domain to lie colinear with the ion conduction pathway, yet recent results demonstrate that the T1 does not contribute to ion permeation. If the crystal structure of the isolated domain represents the T1 domain in a functioning K^+ channel, do the conducting ions circumvent or transverse the T1 domain? To address this question, we made pairs of cysteine mutants predicted to line the subunit-subunit interfaces and expressed these channels in *Xenopus* oocytes. Disulfide cross-links were only observed between residues that formed a hydrogen bond(s) between T1 subunits. Furthermore, we have compared the ion-conducting properties of these channels under reducing and oxidizing conditions. Our results

show that the T1 domain of a functioning K^+ channel is indeed tetrameric, and therefore must hang from the channel, creating "windows" that allow the passage of conducting ions as well as internal pore blockers. This picture is highly reminiscent of the recent high-resolution structure of the nictotinic acetylcholine receptor (Miyazawa et al. 1999. *J. Mol. Biol.* 288:765–786).

34. Access of Protons to the Sodium Channel Pore Monitored with Titratable μ -Conotoxin Derivatives KWOKYIN HUI and ROBERT J. FRENCH, *Department of Physiology and Biophysics, University of Calgary, Calgary, Alberta, Canada*

We have used a pair of derivatives of μ -conotoxin GIIIA, with titratable residues substituted for the critical arginine-13, to obtain an indication of local pH in the Na channel pore. Wild-type toxin causes all-or-none block of single skeletal muscle Na channels, while residue-13 mutants block only partially. Positive residues in position 13 cause more complete block than neutral or negative ones (Hui and French. 2000. *Biophys. J.* 78:86A). The docking site of residue-13 has been identified near the channel's selectivity filter (Chang et al. 1998. *Biochemistry.* 37:4407–4419). Thus, by substituting titratable amino acids for arginine-13 (derivatives R13E and R13H), we generated sensors that should reflect changes in the local pH in the pore as pH varies in the bulk solution. Both binding kinetics and the completeness of single-channel block by these derivatives depended on pH. In general, pH values that favored the neutral form of the residue-13 side chain promoted behavior similar to derivative R13A, with neutral alanine in this position. We postulate that the fractional residual current, F_{res} , through single channels bound by toxin, and the dissociation rate constant, k_{off} , should reflect properties of the toxin-channel bound complex, while the association rate constant, k_{on} , should be determined primarily by the state of the free toxin in solution. The fractional current block by R13E and R13H varied with pH with pKs of 6.9 ± 0.2 and 8.0 ± 0.4 , respectively, whereas for R13A it was independent of pH. The k_{off} s of the titratable mutants had a pK similar to those for the fractional current block. However, their k_{on} s had pKs nearer the nominal values for the side chains of the free amino acids: <5 for R13E, and ≈ 6.5 for R13H. The results are consistent with a local pH in the vestibule of the toxin-bound channel that is ≥ 1.5 U lower than in bulk solution, suggesting that protons are concentrated in the pore vestibule as befits a cation-selective channel. (Supported by the Medical Research Council of Canada, and the Alberta Heritage Foundation for Medical Research.)

35. Polyamines Block Rat Skeletal Muscle (μ 1) Sodium Channels Expressed in HEK293 Cells CHIEN-JUNG HUANG and EDWARD MOCZYDLOWSKI, *Department of Pharmacology, Yale University School of Medicine, New Haven, Connecticut*

Polyamines such as spermidine and spermine are well-known endogenous blockers of inward-rectifier K^+ channels and glutamate receptor channels, but have previously received relatively little attention as possible modulators of voltage-gated Na^+ channels (Na_v). We have demonstrated that polyamines are potent blockers of the μ 1 Na^+ channel expressed in HEK293 cells and that this blocking behavior closely mimics endogenous inward rectification of Na_v current measured in the early phase of current recording in the whole cell voltage-clamp configuration. Under conditions of symmetrical Na^+ concentration, whole-cell

peak current from HEK293 cells stably expressing μ 1 Na_v exhibits a rectification behavior indicative of voltage-dependent block and relief of block at high positive voltage. This blocking behavior progressively disappears as a function of time, but does not completely vanish even after 30 min of recording. This phenomenon suggests that washout of endogenous cellular blocker(s) by the internal pipet solution is relatively slow. Removal of divalent cations (Mg^{2+} , Ca^{2+}) and substitution of HEPES buffer with sodium phosphate in the pipet solution does not remove or prevent this endogenous blocking phenomenon. We hypothesized that this phenomenon is due to internal block by endogenous polyamines. This idea is supported by experiments in which addition of 1 mM spermine or spermidine to the pipet solution results in whole-cell I-V curves with a persistent negative resistance region at positive voltage, similar to that seen immediately after membrane break-in in control cells without added polyamines. To directly investigate the effect of polyamines on Na_v channels and their interactions with the selectivity filter, inside-out macro-patch experiments were performed on HEK293 cells expressing wild-type μ 1 and the K1237A (DEAA) selectivity filter mutant channel using symmetrical Na^+ solutions. Peak I-V relationships up to +200 mV indicate that spermine and spermidine are approximately equipotent in reversibly blocking the wild-type Na_v channel in the concentration range of 1–100 μ M. In contrast, the blocking behavior of spermine and spermidine for the DEAA mutant channel is remarkably different from that of the wild-type channel, exhibiting more pronounced relief of block at high voltage. Spermine appears to be more potent than spermidine in blocking the DEAA mutant channel. In particular, the former polyamine, but not the latter, blocks the DEAA channel in a strongly use-dependent fashion, revealing an underlying structure-activity relationship of polyamine block. Our results support the idea that cellular polyamines are endogenous blockers of Na_v channels and that these organic cations also engage in molecular interactions with the selectivity filter. (Supported by NIH grant GM-51172.)

36. A New Highly Selective Conotoxin from *Conus californicus* that Targets Voltage-gated Neuronal Na^+ Channels of Squid JON-PAUL BINGHAM,*[‡] ALMA BURLINGAME,[‡] EDWARD MOCZYDLOWSKI,* and WILLIAM F. GILLY,[§] **Department of Pharmacology, Yale University, New Haven, Connecticut; †Mass Spectrometry Facility, Department of Pharmaceutical Chemistry, University of California, San Francisco, California; and ‡Hopkins Marine Laboratory, Stanford University, Pacific Grove, California*

Venoms from *Conus*, a carnivorous marine gastropod, are a rich source of peptide toxins that target various ion channels with highly selective subtype specificity. For example, *Conus* snails have provided ω -conotoxins that differentiate the various isoforms of voltage-gated Ca^{2+} channels, α -conotoxins that differentiate between various pentameric isoforms of nictotinic acetylcholine receptor channels, and μ -conotoxins that differentiate muscle, neuronal, and cardiac isoforms of voltage-gated Na^+ channels. In our study of the endemic *Conus* species, *Conus californicus* that is found in cooler waters of the mid coastal region of California, we demonstrated the presence of a new highly selective Na^+ channel toxin present in both the crude duct venom extract and the captive milked venom. Thus far, this novel peptide toxin was found to selectively differentiate between various species isoforms of Na^+ channels. It blocked the voltage-gated Na^+ channel in giant fiber lobe (GFL) of Pacific squid, with an ab-

sence of effect on squid Ca^{2+} and K^{+} currents and the glutamate-activated response in GFL. The lack of an effect on Na^{+} currents of the mollusc *Aplysia californica* also demonstrated its selectivity at a phylogenetic level. By analysis of the captive milked venom by reverse-phase high performance liquid chromatography (RP-HPLC), and electro-spray mass spectrometry (ESMS), we observed that the active peptide was a major constituent in the hydrophobic region of the HPLC profile. However, its concentration in the crude duct venom was relatively minor. Sequential isolation and Edman characterization demonstrated a high number of post-translational modifications, a high percentage of hydrophobic amino acids, and an unusual disulfide framework distinct from other previously reported conotoxins directed against voltage-gated Na^{+} channels (μ -, δ -, and GS-conotoxins). These features provide evidence that this toxin represents a new class of Na^{+} channel conotoxins.

37. Direct Binding of Ca^{2+} by a COOH-terminal Domain of the *Drosophila Slowpoke* BK(Ca) Channel SHUMIN BIAN, ISABELLE FAVRE, and EDWARD MOCZYDLOWSKI, Department of Pharmacology, Yale University School of Medicine, New Haven, Connecticut

Large conductance Ca-activated K-channels (BK) are thought to consist of an NH_2 -terminal membrane domain (Core) and a COOH-terminal Ca-activation domain (Tail). To investigate Ca^{2+} -binding properties of the Tail domain, we expressed in *Escherichia coli* the carboxy-terminal 280 residues of the *Drosophila* BK(Ca) channel (DslO) tagged at the amino terminus with FLAG and (His)₆ epitopes (DslO-C280). DslO-C280 was purified to homogeneity in soluble form starting from a soluble extract of *E. coli* and also from inclusion protein after denaturation and refolding. Ni^{2+} -chelate affinity, anti-Flag immunoaffinity, and high performance size-exclusion chromatography (HPSEC) were used in various purification steps. Purified DslO-C280 tends to form high molecular weight aggregates that can be dispersed by treatment with DTT and mild detergent. The smaller protein species migrate as an apparent mixture of monomer to tetramer on HPSEC. Direct $^{45}\text{Ca}^{2+}$ -binding activity of purified DslO-C280 was demonstrated in $^{45}\text{Ca}^{2+}$ overlay assays with autoradiographic detection. DslO-C280 exhibits robust $^{45}\text{Ca}^{2+}$ -binding activity both in crude and highly purified states. Specificity is demonstrated by $^{45}\text{Ca}^{2+}$ bands for positive controls such as EF-hand Ca^{2+} -binding proteins, calmodulin, calpain, and troponin C, and the absence of such bands for negative controls such as Flag-tagged alkaline phosphatase, trypsin, and various molecular weight standards. Under the same conditions, acidic proteins with a low isoelectric point similar to DslO-C280, such as annexin, glucose oxidase, and ovomucoid, do not exhibit significant $^{45}\text{Ca}^{2+}$ -binding activity. This indicates that $^{45}\text{Ca}^{2+}$ -binding activity in this assay is structure specific and not a general electrostatic association phenomenon. To examine the role of the Ca^{2+} -bowl motif (Schreiber and Salkoff, 1997. *Biophys. J.* 73:1355–1363) in Ca^{2+} binding, a DslO mutant with five consecutive aspartate residues in the Ca^{2+} bowl were changed to asparagine (D5N5). Mutant D5N5 BK(Ca) channels expressed in transiently transfected HEK293 cells exhibited a marked decrease in Ca^{2+} sensitivity in inside-out patch experiments. A corresponding DslO-C280 mutant (D5N5) was constructed, expressed in *E. coli*, and purified. In parallel $^{45}\text{Ca}^{2+}$ overlay assays, the D5N5 mutant (Fig. 1, lanes 2, 4, and 6) has $\sim 35\%$ $^{45}\text{Ca}^{2+}$ -binding activity in comparison with wild-type (lanes 1, 3, and 5) DslO-C280, consistent with an observed decrease in Ca^{2+} sensitivity for activation of functional channels. Our results demonstrate that direct biochemical measurements of Ca^{2+} binding to a COOH-terminal domain of the *Drosophila* BK(Ca) channel

can be correlated with changes in Ca^{2+} -dependent channel activation. (Supported by AHA Postdoctoral Fellowship grants to S. Bian and I. Favre, and NIH grant GM-51172 to E. Moczydlowski.)

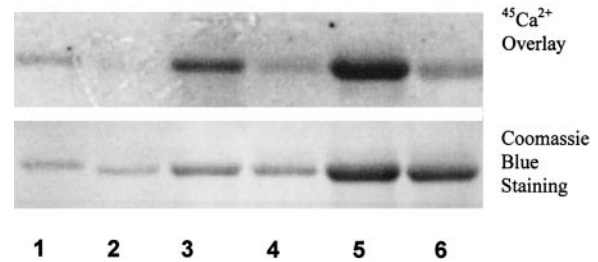


FIGURE 1.

38. Mutations Near the Predicted Catalytic Site of NBD1 in CFTR Subtly Affect Cl^{-} Channel Function PAOLA VERGANI, CLAUDIA BASSO, LÁSZLÓ CSANÁDY, DAVID KOPSCO, ROBERTO SÁNCHEZ, ANDREJ ŠALI, ANGUS C. NAIRN, and DAVID C. GADSBY, The Rockefeller University, New York, New York 10021

CFTR Cl^{-} channels have intrinsic ATPase activity, and hydrolyzable nucleoside triphosphate is needed for channel gating, but the link between ATP hydrolysis and opening, and the precise roles of the two nucleotide-binding domains (NBDs), remain unclear. To assess its contribution to channel activity, we mutated NBD1 on the basis of a model built from crystal structures of related ABC transporter domains, His-P and RbsA. We targeted L435 and F433 (corresponding to residues that interact with the adenine ring of ATP in the crystals), S605 (in a proposed “switch” region), Q493, and S573 (corresponding to putative ligands for the “attacking” water molecule), the Walker B D572 (providing key coordination for the Mg^{2+} ion), and the Walker A lysine K464 (crucial for hydrolysis). Oocytes expressing L435A, L435S, F433A, F433L, S605A, Q493A, S573A, or K464A CFTR mutants all yielded robust forskolin-activated conductance. Furthermore, the open probability (P_o) of L435S, F433A, S605A, or S573A channels was near half maximal at 50 μM [ATP], as in wild-type (WT) channels, but the apparent affinity for ATP, as assessed by P_o , was reduced ~ 1.5 -fold for Q493A and ~ 4 -fold for K464A channels. At saturating [ATP], D572N channels showed a reduced opening rate, but single-channel kinetic parameters were not significantly altered (compared with WT) in Q493A and K464A channels. Orthovanadate, shown to markedly stabilize the open state of WT CFTR, had a far smaller effect on Q493A mutants and did not affect the closing rate of K464A channels. The observed vanadate-induced trapping of $\alpha^{32}\text{P}$ -8-azido-ATP in WT CFTR (apparently in NBD1) is abrogated in mutant Q493A or K464A CFTR. These results suggest that hydrophobic interactions with L435 and/or F433 are not principal determinants of apparent ATP affinity at NBD1 and that ATP is indeed hydrolyzed at NBD1, but that interfering with ATP hydrolysis and/or post-hydrolytic events (K464A, Q493A) at NBD1 affects CFTR channel gating surprisingly little. (Supported by NIH DK51767.)

39. ATP and Calyculin-A Inhibit Dephosphorylation of CFTR in Excised Patches THOMAS J. O'SHAUGHNESSY and WILLIAM W. REENSTRA, Department of Medi-

cal and Clinical Research, Alfred I. duPont Hospital for Children, Wilmington, Delaware

The cystic fibrosis transmembrane conductance regulator (CFTR) is a chloride channel. Activation requires phosphorylation of the R domain, and gating is regulated by ATP hydrolysis at two nucleotide binding domains (NBDs). The relationship between channel activity and R domain phosphorylation is unknown, but higher levels of phosphorylation are thought to increase channel activity. It has been suggested that CFTR dephosphorylation only occurs in the closed state. To test this, CFTR in multichannel cell-attached patches were activated with forskolin. Activated patches were then excised into 0 or 1 mM ATP, or calyculin-A. Patches excised into 0 mM ATP lost 100% of the initial current, and addition of 1 mM ATP restored $8 \pm 3\%$ ($n = 7$) of the initial current. Patches excised into 1 mM ATP retained $29 \pm 6\%$ ($n = 24$) of the initial current; subsequent ATP removal caused the loss of all channel activity, but readdition of 1 mM ATP restored current to the previous level. Patches excised into calyculin-A rapidly lost channel activity, but 1 mM ATP restored $28 \pm 8\%$ ($n = 6$) of the initial current. These results suggest that (a) ATP binding to NBDs inhibits dephosphorylation, and (b) a protein phosphatase associated with CFTR is rapidly lost upon excision.

Since phosphatase inhibitors may selectively dephosphorylate CFTR phosphorylation sites, the phosphorylation states of CFTR excised into ATP and calyculin-A may differ. Since pyrophosphate has been postulated to lock open only highly phosphorylated CFTR, we compared the effect of pyrophosphate on CFTR excised into ATP or calyculin-A. Pyrophosphate increased mean current, current variance, and P_o by similar amounts under both conditions.

Several conclusions are possible. (a) Phosphorylation patterns of CFTR excised into ATP and calyculin-A do not differ. (b) CFTR is dephosphorylated by only one phosphatase in this system. (c) Pyrophosphate increases CFTR activity regardless of phosphorylation state. The later possibility is consistent with experiments in which pyrophosphate locked open channels with an initial $P_o \leq 0.1$. (Supported by the Nemours Foundation, CFF, and the Institute for Human Gene Therapy.)

40. Identification of the Residues Responsible for the Activation of *Xenopus* CFTR by PKC Stimulation B. BUTTON, G.A. ALTENBERG, and L. REUSS, *Department of Physiology and Biophysics, University of Texas Medical Branch, Galveston, Texas*

Activation of the CFTR chloride channel requires phosphorylation of its regulatory domain (R domain) by protein kinase A. We have previously demonstrated (Button et al. 2000. *FASEB J.* 14:A336) that, contrary to the human CFTR (hCFTR), the *Xenopus* homologue of CFTR (XCFTR) expressed in *Xenopus* oocytes can be fully activated by both PKC and PKA. Expression experiments with hCFTR-XCFTR chimeras have established that the R domain of XCFTR accounts for the differences in activation of human and *Xenopus* CFTRs by PKC-mediated phosphorylation. Two PKC consensus phosphorylation sites are expressed in both XCFTR and hCFTR, whereas the other two are unique to XCFTR. To determine the roles of these sites in the PKC-mediated activation of XCFTR, mutations (Ser/Thr to Ala) were carried out individually or in combination. Substitution of the conserved PKC sites (Ser⁶⁸⁶ and Ser⁷⁹⁰) did not influence the activation of XCFTR by PKC. However, substitution of the unique sites (Thr⁶⁶⁵ and Ser⁶⁹⁴) abolished the effect of PKC stimulation, producing a

phenotype similar to that of hCFTR. Substitution of single unique sites resulted in a graded response to PKC stimulation, with Thr⁶⁶⁵ as the most important for the response. These results suggest that activation of XCFTR by PKC-mediated phosphorylation involves critical sites that are unique to XCFTR, rather than the net charge of the R domain. These data also suggest a hierarchy of PKC-mediated phosphorylation in the activation of XCFTR. (Supported by NIH grant DK-38734.)

41. Increased Phosphorylation of CFTR Increases Apparent Affinity to ATP GEORG NAGEL and TANJEF SZEL-LAS, *Max-Planck-Institut für Biophysik, D-60596 Frankfurt, Germany*

The epithelial chloride channel CFTR is regulated by phosphorylation by kinases and nucleotides interacting with the two nucleotide binding domains. Giant excised inside-out membrane patches from *Xenopus lewis* oocytes expressing human CFTR were continuously perfused. Previously, patches were tested for their chloride conductance in response to the transient application of (soluble) catalytic subunit of cAMP-dependent protein kinase (PKA) and different concentrations of ATP, yielding a K_m for ATP of 80 μ M (Weinreich et al. 1999. *J. Gen. Physiol.* 114:55-70). Now we've engineered a membrane-bound PKA (BR-PKA) by fusing the catalytic subunit of PKA to the COOH terminus of bacteriorhodopsin (BR). Coexpression of BR-PKA with CFTR led to a distinctly increased apparent affinity for ATP with a K_m of 40 μ M. When coexpressing the (naturally) membrane-bound cGMP-dependent protein kinase (cGK) II with CFTR, we again found an increased apparent affinity for ATP ($K_m = 30 \mu$ M in the continuous presence of cGMP). These membrane-bound protein kinases prevented in most cases the usual rundown of CFTR activity, most probably by counteracting endogenous membrane-bound phosphatases. We therefore conclude that the increased phosphorylation of CFTR by continuously active membrane-bound protein kinases increases the apparent affinity of CFTR to ATP. (Supported by DFG and MPG.)

42. Nucleotide Binding to the First Nucleotide-binding Domain of P-Glycoprotein DENISE M. WILKES and GUILLERMO A. ALTENBERG, *Department of Physiology and Biophysics, University of Texas Medical Branch, Galveston, Texas*

P-glycoprotein (Pgp) uses the energy from ATP hydrolysis to transport drugs across cell membranes. Nucleotide binding and hydrolysis occur at the nucleotide-binding domains (NBDs). We explored the binding selectivity of the first Pgp NBD (NBD1) fused to the COOH terminus of maltose-binding protein. The NBD was expressed in *Escherichia coli* and purified to 90-95% based on its affinity for amylose. The fluorescence of the ATP analogue trinitrophenyl ATP (TNP-ATP) increased upon binding to NBD1, and the displacement of TNP-ATP from NBD1 was used to assess selectivity. The emission spectrum of TNP-ATP bound to NBD1 showed a shift to shorter wavelengths, indicating that the bound TNP-ATP is in a more hydrophobic environment. The TNP-ATP K_d was 7 μ M, and it was displaced by ATP > ADP > pyrophosphate (PP_i) > AMP. NBD1 contains conserved sequences, the motifs A, B, and C. To determine the contribution of the conserved motif A sequence, we studied an NBD1 fragment of about half-size (MARD), comprising motif A, but not motifs B and C. This protein bound TNP-ATP with reduced affin-

ity ($K_d = 16 \mu\text{M}$), and altered affinity profile (ATP > PP_i > ADP > AMP). These results suggest that motif A acts as a PP_i binding site. Substitution of the motif A lysine of MARD resulted in a further decrease in TNP-ATP affinity and loss of the PP_i binding profile (ATP > ADP > PP_i). The notion that motif A acts as a PP_i binding site was confirmed by studies on a motif A deletion mutant of NBD1. This protein bound TNP-ATP with reduced affinity ($K_d > 50 \mu\text{M}$), but did not behave as a PP_i binding site because it showed the same relative affinities similar to those of the complete NBD1. We conclude that: (a) the nucleotide binding pocket of Pgp NBD1 is relatively hydrophobic, (b) the conserved motif A is a PP_i binding site with lysine⁴³³ as the critical residue, and (c) regions beyond motif A are required for the selectivity of the NBD for different nucleotides. (Supported in part by NIH grant CA-72783.)

43. Adenophostin A Induces a Novel Gating Mode of the Inositol (1,4,5)-Trisphosphate Receptor ELENA NOSYREVA,* RACHEL D. MARWOOD,[†] SVETLANA SEMYONOVA,* VITALIE LUPU,* ALAN V. SMRCKA,[§] BARRY V.L. POTTER,[†] and ILYA BEZPROZVANNY,* *Department of Physiology, University of Texas Southwestern Medical Center at Dallas, Dallas, Texas; [†]Wolfson Laboratory of Medicinal Chemistry, Department of Pharmacy and Pharmacology, University of Bath, Claverton Down, Bath, United Kingdom; and [§]Department of Pharmacology and Physiology, University of Rochester School of Medicine and Dentistry, Rochester, New York

The inositol (1,4,5)-trisphosphate receptor (InsP₃R) plays a key role in intracellular Ca²⁺ signaling. Binding of InsP₃ is required for InsP₃R activation. InsP₃R is a tetramer with each subunit containing a highly selective InsP₃ binding site. In this paper, we describe the effects of a novel superpotent InsP₃R agonist, Adenophostin A (AdA), on rat cerebellar InsP₃R incorporated into planar lipid bilayers. We show that (a) AdA activates rat cerebellar InsP₃R in planar lipid bilayers at ~10-fold lower concentrations than InsP₃; (b) two populations of InsP₃R are observed in the presence of AdA, each displaying a distinct gating mode, the "normal mode" (predominant) is characterized by brief openings (~5 ms) and low open probability ($P_o = 5\text{--}10\%$), the "bursting mode" (rare) is characterized by 20–30-s bursts of long InsP₃R channel openings (~250 ms) with extremely high open probability ($P_o > 95\%$) within a burst; (c) InsP₃R gating in the presence of AdA can be converted from normal to a bursting mode by synergistic action of monoclonal anti-phosphatidylinositol (4,5)-bisphosphate antibody (PIP₂Ab) and recombinant phospholipase C β (PLCβ), but not by either agent alone; and (d) bursting behavior in identical conditions is not observed with InsP₃.

Based on these data, we propose (a) that a bursting mode of InsP₃R gating results from AdA association with all four ligand-binding sites of InsP₃R tetramer; (b) that an adequate InsP₃R gating model that describes bursting gating must combine elements of the Monod-Wyman-Changeux symmetrical model (Monod et al. 1965. *J. Mol. Biol.* 12:88–118) with the sequential model (Koshland et al. 1966. *Biochemistry.* 5:365–385); (c) that binding of AdA to all four ligand-binding sites of rat cerebellar InsP₃R is in most cases prevented by InsP₃R-tethered endogenous PIP₂ (Lupu et al. 1998. *J. Biol. Chem.* 27:14067–14070), resulting in a normal InsP₃R gating mode; and (d) that bursting and normal InsP₃R gating modes observed in vitro correspond, respectively, to physiological gating modes of submembrane and intracellular InsP₃R

in situ. [Supported by the AHA, the Robert Welch Foundation, and NIH grant NS38082 (I. Bezprozvanny), NIH grant GM53536 (A.V. Smrcka), Wellcome Trust grant 045491 (B.V.L. Potter), and the Wellcome Trust Prize Studentship (R.D. Marwood).]

44. Adenophostin A and Inositol 1,4,5-Trisphosphate Confers Distinct Calcium Dependencies of Inositol Trisphosphate Receptor Gating, Dependent on ATP DON-ON DANIEL MAK, SEAN McBRIDE, and J. KEVIN FOSKETT, Department of Physiology, University of Pennsylvania, Philadelphia, Pennsylvania

Adenophostin A (AdA), a fungal metabolite with structural similarity to inositol 1,4,5-trisphosphate (InsP₃), binds the ubiquitous intracellular InsP₃ receptor (InsP₃R) with high affinity (100× that of InsP₃) and stimulates Ca²⁺ release by the InsP₃R channel. Because calcium signals elicited by AdA are distinct from those elicited by InsP₃, we studied the effects of AdA on the single-channel activities of the type I InsP₃R at various cytoplasmic free Ca²⁺ and ATP concentrations by patch clamping isolated *Xenopus* oocyte nuclei. In the presence of 0.5 mM free ATP, the biphasic Ca²⁺ dependence of InsP₃R channel gating was indistinguishable for channels activated by either saturating [AdA] (100 nM) or [InsP₃] (10 μM), with maximum channel open probability (P_{max}) of 0.8, half-maximal activating [Ca²⁺] (K_{act}) of 210 nM, activation Hill coefficient (H_{act}) of 2, half-maximal inhibitory [Ca²⁺] (K_{inh}) of 50 μM, and inhibition Hill coefficient (H_{inh}) of 4. Like InsP₃, AdA activated the channel by increasing K_{inh} , but with a potency ~65× that of InsP₃. In the absence of ATP, Ca²⁺ activation of InsP₃R stimulated by either AdA or InsP₃ was likewise similar, with K_{act} of 500 nM and H_{act} of 2.4. Both InsP₃ and AdA activated the channel by increasing K_{inh} . However, in the absence of ATP, whereas InsP₃R gating activated by InsP₃ still had a P_{max} of 0.8, InsP₃R activated by AdA could only attain a P_{max} of 0.4. Moreover, in the absence of ATP, InsP₃ and AdA activated the InsP₃R with comparable potency. This suggests that the high potency of AdA to activate InsP₃R channel is not due to simultaneous interaction of the InsP₃-like triple phosphoryl groups and adenosine moiety of AdA with the InsP₃- and ATP-binding sites, respectively, of the InsP₃R channel. Instead, ATP binding to the InsP₃R has an allosteric effect on the structure of the InsP₃-binding site of the channel, favoring AdA binding. Furthermore, the unique dependence on ATP of the P_{max} activated by AdA indicates that in the absence of ATP, the InsP₃R channel is activated by AdA to a state fundamentally different from that activated by InsP₃. (Supported by NIH grant GM-56328.)

45. Consequences of Mutations in Stalk Segment S5 of the Sarcoplasmic Reticulum Ca²⁺-ATPase THOMAS LYKKE-MØLLER SØRENSEN and JENS PETER ANDERSEN, Department of Physiology, University of Aarhus, Aarhus, Denmark

The Ca²⁺-ATPase of sarcoplasmic reticulum actively transports calcium ions using energy derived from ATP. Structural studies of the Ca²⁺-ATPase have revealed a large cytoplasmic head, which through a stalk is connected with the transmembrane domain. The tight coupling between the catalytic and vectorial processes, associated with the cytoplasmic head and the membrane domain, respectively, is dependent on intramolecular signaling through the interconnecting stalk. Site-directed mutagenesis studies as well as modeling of the 3-D structure point to stalk seg-

ments S4 and S5, connected with the 4th and the 5th transmembrane segments, respectively, as the principal mediators of this communication. Mutations to residues in stalk segment S4 lead to impairment of the Ca^{2+} -translocation capabilities of the enzyme, suggesting an important role of this segment in transmission of ATP-derived energy required in the membrane domain for Ca^{2+} translocation. The function of stalk segment S5 is less well understood. We have previously demonstrated that replacement of Lys⁷⁵⁸ with isoleucine leads to a concurrent increase in the rate of dephosphorylation and a decrease in the rate of the Ca^{2+} -binding transition (Sørensen et al. 1997. *J. Biol. Chem.* 48: 30244–30253).

In the present study, several highly conserved residues in stalk segment S5 were substituted by site-directed mutagenesis. At 37°C, the rate of ATP hydrolysis was reduced, relative to wild type, in mutants Val⁷⁴⁴→Gly, Val⁷⁴⁷→Ala, Lys⁷⁵⁸→Val, and Arg⁷⁶²→Ile, and activation upon addition of Ca^{2+} ionophore was not seen for Lys⁷⁵⁸→Val or Arg⁷⁶²→Ile, although either of these mutants transported Ca^{2+} . At 0°C, the rate of the Ca^{2+} -binding transition was enhanced in mutants Ile⁷⁴³→Ala, Val⁷⁴⁷→Ala, Glu⁷⁴⁹→Ala, Met⁷⁵⁷→Gly, and Gln⁷⁵⁹→Ala, and decreased in mutants Asp⁷³⁷→Ala, Asp⁷³⁸→Ala, Ala⁷⁵²→Leu, and Lys⁷⁵⁸→Val. Mutant Gly⁷⁵⁰→Ala showed a >15-fold increase in the rate of Ca^{2+} dissociation. The rate of dephosphorylation was 20–40-fold increased in mutants Ile⁷⁴³→Ala, Tyr⁷⁵⁴→Ala, and Lys⁷⁵⁸→Val, in contrast to a 1.5–2-fold decrease in mutants Val⁷⁴⁴→Gly, Ala, Val⁷⁴⁷→Ala, and Ala⁷⁵²→Leu. Mutants with alterations to Arg⁷⁵¹ were either not expressed at a significant level or were completely nonfunctional. These findings suggest that S5 plays a key role in mediating communication between the cation binding pocket and the catalytic domain, and that Arg⁷⁵¹ in particular is important for both structural and functional integrity of the enzyme.

46. Mutational Analysis of the Role of Thr353 in the Catalytic Activity and Conformational Changes of the Sarco(endo)plasmic Reticulum Ca^{2+} -ATPase JOHANNES D. CLAUSEN and JENS PETER ANDERSEN, *Department of Physiology, University of Aarhus, Aarhus, Denmark*

The Ca^{2+} -ATPase of the sarcoplasmic reticulum (SR) belongs to the family of P-type ATPases that are characterized by a unique reaction cycle involving phosphorylation and dephosphorylation of a conserved aspartic acid residue. Thr353 of the SR Ca^{2+} -ATPase is located close to the phosphorylated residue, Asp351, and is highly conserved within the family of P-type cation pumps. It is, however, not conserved within the whole haloacid HAD superfamily of hydrolases that, besides P-ATPases, comprises phosphatases, epoxide hydrolases, and haloacid dehalogenases. In contrast to the haloacid dehalogenase and the epoxide hydrolase, the P-ATPases and the phosphatases require Mg^{2+} or a divalent cation substitute for activity. Recently, it was suggested on the basis of structural alignment of HAD superfamily members that the main chain carbonyl corresponding to Thr353 contributes to coordination of the catalytic Mg^{2+} (Ridder and Dijkstra. 1999. *Biochem. J.* 339:223–226). In the present work, we have studied the functional consequences of various mutations to Thr353. We find that the ability to undergo phosphorylation by either ATP or P_i is markedly reduced for several Thr353 mutants. In mutant Thr353→Val, the rate constant for phosphorylation with 5 μM MgAT^{32}P at 25°C is 500-fold reduced relative to the wild type, whereas the effect is even more pronounced in mutant Thr353→Cys and less so in mutant Thr353→Ser. Studies of dephosphorylation kinetics after chase of the phosphoenzyme with

nonradioactive ATP and ADP show that the conformational transition between the ADP-sensitive ($E_1\text{P}$) and the ADP-insensitive ($E_2\text{P}$) phosphoenzyme intermediates is blocked in these mutants. In addition, we show that the rate of forward dephosphorylation of mutant Thr353→Ser accumulated on the $E_2\text{P}$ form is accelerated relative to the wild type. Our results are in agreement with a role for Thr353 in coordination of the catalytic Mg^{2+} ion. (Supported by the Danish Medical Research Council, and the NOVO Nordisk Foundation, Denmark.)

47. Protection of Solubilized Sarcoplasmic Reticulum Ca^{2+} Transport ATPase by an Amphipathic Polymer, Amphipol A8-35 PHILIPPE CHAMPEIL,* THIERRY MENGUY,* CHRISTOPHE TRIBET,† JEAN-LUC POPOT,§ and MARC LE MAIRE,* *Unité de Recherche Associée 2096 (Centre National de la Recherche Scientifique et Commissariat à l'Energie Atomique) and Section de Biophysique des Protéines et des Membranes, CEA Saclay, France; †Unité Mixte de Recherche 7615 (Centre National de la Recherche Scientifique, Université Paris VI and Ecole Supérieure de Physique et Chimie Industrielles), Paris, France; and §Unité Propre de Recherche 9052 (Centre National de la Recherche Scientifique) and Institut de Biologie Physico-Chimique, Paris, France

Amphipols are short-chain amphipathic polymers designed to keep membrane proteins soluble in aqueous solutions. We have evaluated the effects of the interaction of amphipols with sarcoplasmic reticulum Ca^{2+} -ATPase in either a membrane-bound or a soluble form. If the addition of amphipols to detergent-solubilized ATPase was followed by removal of detergent, soluble complexes formed, but these complexes retained poor ATPase activity, were not very stable upon long incubation periods, and at high concentrations they experienced aggregation. Nevertheless, adding excess detergent to diluted detergent-free ATPase/amphipol complexes incubated for short periods immediately restored full activity to these complexes, showing that amphipol had protected solubilized ATPase from the rapid and irreversible inactivation that otherwise follows detergent removal. Amphipols also protected solubilized ATPase from the rapid and irreversible inactivation observed in detergent solutions if the ATPase Ca^{2+} binding sites remain vacant. Moreover, in the presence of Ca^{2+} , amphipol/detergent mixtures stabilized concentrated ATPase against inactivation and aggregation, whether in the presence or absence of lipids, for much longer periods of time (days) than detergent alone. Our observations suggest that mixtures of amphipols and detergents are promising media for handling solubilized Ca^{2+} -ATPase under conditions that would otherwise lead to its irreversible denaturation and/or aggregation.

48. Chelator Enhancement of Active Ca Transport R.F. ABERCROMBIE, X.-J. MENG, J.E. MOORE, and K.M. WELLS, *Department of Physiology, Emory University, Atlanta, Georgia*

Much effort has been devoted to uncovering the biophysical mechanisms associated with energy-coupled active Ca transport. The issue presented here, which has received relatively little attention, concerns the mechanism(s) of physical delivery of calcium ions to their transport sites on the Ca-ATPase. Evidence suggests that if transport is below its maximum rate and free calcium is fixed, mobile Ca chelators (either native chelators such

as calbindin and parvalbumin, or synthetic chelators such as EGTA) increase transport, both on intracellular- and plasma membrane-type calcium pumps (see, for example, Berman. 1982. *J. Biol. Chem.* 257:1953; Timmermans et al. 1995. *J. Nutr.* 125:1981S). These observations, however, oppose the theoretical expectation that Ca chelators should be unable to release calcium with enough speed to make much difference in the “loading” step of a “Ca-starved” transport reaction. It must be concluded that we do not understand the mechanisms by which calcium transport sites become loaded or how chelators enhance a calcium loading/transport reaction. Such mechanisms, however, may be especially important for the transport activity of cells that must move large amounts of calcium, such as renal and intestinal epithelial cells and bone resorbing cells, or in certain types of myocytes and neurons that may need to transport calcium quickly into intracellular storage compartments.

We have done experiments to examine the role of chelators in calcium transport in neurons. Microsomes isolated from rat brain accumulated ^{45}Ca in a free (ionized) Ca concentration ($[\text{Ca}^{2+}]$)- and ATP-dependent manner. This accumulation was inhibited by thapsigargin, and was insensitive to mitochondrial inhibitors or to agents such as digitonin that selectively permeabilize plasma-membrane vesicles. Thus, these microsomes likely contain mainly endoplasmic reticular membranes. Adding the synthetic calcium chelator EGTA or the native Ca chelator parvalbumin increased the initial rate of uptake into the microsomes at a fixed $[\text{Ca}^{2+}]$. The maximal uptake rate found in the presence of EGTA could also be achieved without chelator if $[\text{Ca}^{2+}]$ was high enough. Spectrofluorometric records of free Ca^{2+} in microsome suspensions containing $1.5\ \mu\text{M}$ fura-2 also show that when $15\ \mu\text{M}$ EGTA is present, the microsomal Ca uptake rate is greater. A theoretical analysis suggests that chelator facilitation of calcium flux down a diffusion gradient to a “Ca-starved” pump site is inadequate to explain these observations.

49. Helix Packing of the Cardiac Sodium–Calcium Exchanger: Proximity of Transmembrane Segments 2, 3, and 7 ZHIYONG QIU, DEBORA A. NICOLL, and KENNETH D. PHILIPSON, *Department of Physiology, University of California at Los Angeles, Los Angeles, California*

In a revised topological model of the cardiac $\text{Na}^+\text{-Ca}^{2+}$ exchanger, the exchanger contains nine transmembrane segments (TMSs) and two possible re-entrant loops. The TMSs form two clusters separated by a large intracellular loop (loop f) between TMS5 and TMS6. We have combined cysteine mutagenesis and oxidative crosslinking to study proximity relationships of TMSs in the exchanger. Pairs of cysteines were reintroduced into a cysteine-less exchanger, one in a TMS in the NH_2 -terminal cluster (TMSs 1–5) and the other in a TMS in the COOH -terminal cluster (TMSs 6–9). The mutant exchanger proteins were expressed in HEK293 cells and disulfide bond formation between introduced cysteines was analyzed by gel mobility shifts (Philipson et al. 1988. *Biochim. Biophys. Acta.* 945:298–306). Western blots showed that S117C/V804C, A122C/Y892C, C151/T815C, and C151/A821C mutant proteins migrated to 120 kD under reducing conditions and displayed a partial mobility shift to 160 kD under nonreducing conditions. This indicates the formation of a partial disulfide bond between these paired cysteine residues. Cu-phenanthroline and crosslinker α -PDM enhanced the mobility shift to 160 kD. Our data suggest that TMS7 is close to TMS3 near the intracellular side of the membrane and is in the vicinity of TMS2 at the extracellular end of the helices. Also, TMS2 must

adjoin TMS8. This initial packing model of the exchanger also brings two functionally important domains in the exchanger, the $\alpha 1$ - and $\alpha 2$ -repeats, close to each other. Mutant proteins C151/T815C and C151/A821C had increased activities when analyzed using a whole-cell ^{45}Ca uptake assay. The inter-TMS disulfide bond formation between TMS3 and TMS7 may facilitate a more active conformation for ion transport. (Supported by NIH grant HL-49101 and a grant from American Heart Association, Western States Affiliate.)

50. Mitochondrial Flickers Occur in the Absence of Ca^{2+} Sparks in Smooth Muscle Cells CATHERINE M. O'REILLY, ROBERT M. DRUMMOND, KEVIN E. FOGARTY, RICHARD A. TUFT, and JOHN V. WALSH, JR., *Biomedical Imaging Group and Department of Physiology, University of Massachusetts Medical Center, Worcester, Massachusetts*

The potential sensitive fluorescent indicator, tetramethylrhodamine ethyl ester perchlorate (TMRE), was used to measure mitochondrial membrane potential ($\Delta\Psi\text{m}$) in freshly isolated smooth muscle cells from the stomach of *Bufo marinus*. 3-D imaging using a digital imaging system with high temporal and spatial resolution disclosed mitochondria of varying length with their long axis running parallel to the longitudinal axis of the cell. Repeated imaging (one 3-D set every 5 s) revealed spontaneous “flickers” in the TMRE fluorescence that signal transient depolarizations in individual mitochondria. In these same cells, spontaneous Ca^{2+} “sparks” due to transient, localized release of Ca^{2+} from the sarcoplasmic reticulum (SR) through ryanodine receptors (RyRs) have been previously characterized in some detail (ZhuGe et al. 1999. *J. Gen. Physiol.* 113:215–228). The aim of this study was to determine whether Ca^{2+} sparks cause mitochondrial flickers in these smooth muscle cells. Application of $200\ \mu\text{M}$ caffeine to smooth muscle cells resulted in an increase in the mitochondrial flickers. However, neither the basal flicker rate nor the caffeine-stimulated flickers were inhibited by ryanodine ($50\text{--}100\ \mu\text{M}$). Spontaneous flickers were also observed in cells in which stable, whole-cell patch recordings were established at a holding potential of 0 mV. In the presence of $5\ \mu\text{M}$ thapsigargin, the cells were exposed to 20 mM caffeine for 5 s to deplete SR Ca^{2+} . In the continuing presence of thapsigargin, mitochondrial flickers were recorded at 0.5, 5, and 10 min after the 5-s caffeine application—times when, as demonstrated previously (Drummond et al. 2000. *J. Physiol.* 522:375–390), the Ca^{2+} concentration within the mitochondria has returned to resting levels. This study provides evidence that transient changes in $\Delta\Psi\text{m}$ signaled by mitochondrial flickers can occur in the absence of release of Ca^{2+} from SR in smooth muscle cells. (Funded by NIH grant HL61297 to J. Walsh.)

51. Initial Test of “P-loop Model” for P-type Pumps LARRY D. FALLER,* VLADIMIR N. KASHO,* DAVID J. KANE,*† EMAD ELQUZA,† and ROBERT A. FARLEY,† **Digestive Diseases Research Center, University of California, Los Angeles, and Veterans Administration, Greater Los Angeles Healthcare System, Los Angeles, California; and †Department of Physiology and Biophysics, University of Southern California School of Medicine, Los Angeles, California*

We have proposed a model for part of the catalytic site of P-type pumps in which arginine (R) in one of the six conserved signature sequences for P-type pumps is aligned with lysine (K) in

the P-loop of P-loop-containing nucleotide triphosphate hydro-lases (Smirnova et al. 1998. *FEBS Lett.* 431:309–314). The model originated with evidence from site-directed mutagenesis that the carboxyl group in the DPPR sequence of Na,K-ATPase binds Mg^{2+} (Farley et al. 1997. *Biochemistry.* 36:941–951) and assumes that the catalytic site of P-type pumps evolved from enzymes that catalyze phosphoryl group transfer. The function of the positively charged amino group in P-loops is to bind phosphate, polarizing the α -phosphorus–oxygen bond and facilitating nucleophilic attack upon phosphorus. Therefore, the prediction that the positive charge in position 596 (human α 1 subunit) is important for function was tested by expressing the mutants R596K, R596Q, R596A, R596G, and R596E in yeast membranes and evaluating their ability to catalyze phosphorylation by inorganic phosphate (P_i) via ^{18}O exchange measurements. R596K, in which the positive charge is retained, resembled wild type. Substitution of a negative charge (R596E) resulted in complete loss of activity. The remaining mutants with neutral side chains had lowered affinity for P_i and altered isotopomer distributions, consistent with an increased P_i -off rate. Therefore, mutations of both D and R strengthen our hypothesis that the DPPR peptide in Na,K-ATPase functions like the DEGK peptide in the P-loop of adenylosuccinate synthetase, for example. (Supported by NIH grant DK52802.)

52. Mutations in the S3 Domain of the Rat Kidney Na^+,K^+ -ATPase Displace the E_1 - E_2 and E_1P - E_2P Conformational Equilibria in Favor of the E_1 and E_1P Forms
MADS TOUSTRUP-JENSEN, MAJBRIIT HAUGE, and BENTE VILSEN, *Department of Physiology, University of Aarhus, Aarhus, Denmark*

Gly263 located at the boundary between the β -strand sector and the third stalk helix (S3) in the small cytoplasmic domain of rat kidney Na^+,K^+ -ATPase is highly conserved within the family of P-type ATPases. Mutants in which Gly263 or the juxtaposed Arg264 had been replaced by alanine were expressed at high levels in COS cells and characterized functionally. Titrations of Na^+ , K^+ , ATP, and vanadate dependencies of Na^+,K^+ -ATPase activities showed changes in the apparent affinities relative to wild type that could be accounted for by a displacement of the E_1 - E_2 conformational equilibrium in favor of E_1 .

Studies of ADP sensitivity of the phosphoenzyme formed at conditions where the wild type accumulates mainly in the E_2P form showed a more than twofold reduction in the amount of E_2P compared with the wild type. This is in accordance with measurements showing a strongly reduced K^+ sensitivity of the phosphoenzyme in the mutants compared with the wild type. Dephosphorylation studies carried out after phosphorylation in the presence of 600 mM Na^+ demonstrated that the E_1P phosphoenzymes of the mutants decayed slowly, relative to wild type after a downward jump in salt concentration and chase with ATP and K^+ , indicating that the $E_1P \rightarrow E_2P$ conversion rate is reduced in the mutants. This finding was independent of whether the experiments were carried out at 0°C (using a manual mixing technique) or at 25°C (on a millisecond time scale using a quench flow machine). These experiments are all in accordance with an increased stability of the E_1P form relative to E_2P in the mutants.

Measurement of the time course of phosphorylation after addition of [γ - ^{32}P]ATP, oligomycin, and Na^+ to enzyme preincubated with 8 mM K^+ demonstrated that, in the mutants, only 45–70% of the enzyme had formed the K^+ -occluded $E_2(K_2)$ intermediate during the preincubation versus close to 100% in the wild

type, and the rate of deocclusion was enhanced 4–19-fold in the mutants relative to the wild type. This is in accordance with an increased stability of the E_1 form relative to E_2 in the mutants. Using the quench flow technique, it was shown that the phosphorylation rate ($E_1 \rightarrow E_1P$) of the mutants is identical to that of the wild type. Thus, it is concluded that the E_1 and E_1P forms are stabilized in both mutants relative to the wild type due to a decrease in the $E_1P \rightarrow E_2P$ conversion rate and an increase in the rate of K^+ deocclusion, $[K_2]E_2 \rightarrow E_1$. All the above described effects were more pronounced for the Gly263 \rightarrow Ala substitution compared with the more drastic Arg264 \rightarrow Ala substitution, indicating that the flexibility produced by the small side chain of glycine is important for the $E_1/E_1P \rightarrow E_2/E_2P$ transitions of the enzyme.

53. Secondary Structure of the Fifth Transmembrane Segment of the Na,K-Pump α Subunit: A Cysteine Scanning Study
SAÏDA GUENNOUN and JEAN-DANIEL HORISBERGER, *Institute of Pharmacology and Toxicology, University of Lausanne, Lausanne, Switzerland*

To study the structure of the cation pathway across the Na,K-pump, we applied the substituted cysteine accessibility method (Sahin-Toth and Kaback. 1993. *Prot. Sci.* 2:1024–1033) to the putative 5th transmembrane segment of the α subunit of the *Bufo marinus* Na,K-ATPase. Each amino acid residue of this segment, from position K774 to A796, was mutated to a cysteine. When expressed in *Xenopus* oocytes, all the mutants produced measurable electrogenic Na,K-pump activity of various amplitudes (from 10 to 150% of the wild-type value). Only the most extracellular amino acid substitution mutant (A796C) was inhibited by extracellular methanethiosulfonate cysteine reagents in the native Na,K-pump. However, after treatment with palytoxin, which transforms the Na,K-pump into a nonselective cation channel (Wang and Horisberger. 1997. *FEBS Lett.* 409:391–395), six other positions (Y778, L780, S782, P785, E786, and L791) distributed along the whole length of the segment became readily accessible to 2-aminoethyl methanethiosulfonate (MTSEA), as shown by a >50% inhibition of the palytoxin-induced conductance by a 2-min exposure to 100 μ M MTSEA. Three of these residues (Y778, S782, and E786) were already known to be important for cation binding (Pedersen et al. 1998. *Biochemistry.* 37:17818–17827; Vilsen. 1999. *Biochemistry.* 38:11389–11400). It is therefore likely that the pore of the palytoxin-induced channel shares a common structure with the cation binding sites. The accessible residues are not located on the same side of an α -helical model, but the pattern of reactivity rather suggests a β -sheet structure for the inner third of this putative transmembrane segment, a hypothesis that is also supported by protein secondary structure prediction programs. These results provide a first evidence of the relative orientation of amino acid residues in the 5th transmembrane segment and outline their contribution to the cation pathway across the Na,K-ATPase. (Supported by the Swiss FNRS, grant 31-45867.95.)

54. Na,K-ATPase α - and β -Subunit Expression in Insect Cells: Functionally and Immunologically Tracking Through the ER, Golgi, and PM
CRAIG GATTO,*† SCOTT M. McLOUD,* and JACK H. KAPLAN,*
*Department of Biochemistry & Molecular Biology, Oregon Health Sciences University, Portland, Oregon; and †Department of Biological Sciences, Illinois State University, Normal, Illinois

The Na,K-ATPase is an α/β heterodimer with 10 transmembrane segments (Hu and Kaplan. 2000. *J. Biol. Chem.* In press) in the α -subunit and one such segment in the β -subunit. It is the plasma membrane enzyme responsible for the active transport of Na and K and exists in nearly all eukaryotic cells. However, it has been shown that some insect cells (e.g., *Sf-9* and Hi5 cells) have no (or extremely low) Na,K-ATPase. We expressed sheep kidney Na,K-ATPase in Hi5 cells via the Bac-to-Bac baculovirus system (GIBCO BRL). Log-phase Hi5 cells were infected with viral stocks (MOI = 10–15) and harvested at various times after infection (24–72 h). Cells were collected, disrupted, and cell debris removed by centrifugation. The endoplasmic reticulum (ER), golgi apparatus, and plasma membrane (PM) fractions were then separated on a sucrose gradient. The three separate fractions were each analyzed for specific membrane-marker enzyme activities to assess their purity (i.e., glucosidase, ER; mannosidase, Golgi; alkaline phosphodiesterase, PM). Characteristics of Na pump function (i.e., ATPase activity, [^3H]ouabain binding, turnover number, and K^+ dependence) were measured for each fraction at various post-infection times. We found an increase in expression up to ~ 72 h after infection with no significant increases beyond 72 h. In addition, comparisons between functional Na,K-ATPase between the three membrane pools revealed no significant differences. Interestingly, quantitative electroblot analysis suggests that, in our experiments, a high percentage of the expressed Na,K-ATPase remains functional in contrast to several reports claiming that baculovirus expression routinely yields 5% or less functional molecules. We also investigated how the α - and β -subunits were individually processed by Hi5 cells expressing each one alone. We found that the β -subunit alone is produced and processed comparably to the α/β complex. In contrast, the α -subunit undergoes considerable degradation within the ER and Golgi in the absence of the β -subunit. Although there is a small fraction of the α -subunit alone ($\leq 1\%$) that trafficks to the PM, the presence of the α -subunit alone in the PM has been described previously in *Sf-9* cells using immunocytochemistry (Blanco et al. 1994. *J. Biol. Chem.* 269:23420–23425). This is the first report of fractionation and characterization of Na,K-ATPase in intracellular membranes and indicates that the Na,K-ATPase, once assembled, undergoes no further functional modification en route to the PM. (Supported by NIH grants HL30315 to J.H. Kaplan and HL09972 to C. Gatto.)

55. Interaction between Palytoxin and Endogenous Na/K Pumps in HEK293T Cells and Guinea-Pig Ventricular Myocytes PABLO ARTIGAS,* CLAUDIA BASSO,* MIGUEL HOLMGREN,[‡] and DAVID C. GADSBY,* *Laboratory of Cardiac/Membrane Physiology, The Rockefeller University, New York, New York 10021; and [‡]Department of Neurobiology, Harvard Medical School, Boston, Massachusetts*

Palytoxin (PTX) acts on the Na/K pump to produce a nonselective cation conductance. In HEK293T cells (at ~ 22 – 25°C), voltage clamped and internally dialyzed via low-resistance pipettes with MgATP-containing solution, exposure to 0.1–500 nM PTX induced the conductance regardless of whether the principal intracellular and/or extracellular cation was Na^+ , K^+ , or NMDG $^+$. The rate of conductance activation increased with [PTX], but was maximal ($0.3 \pm 0.1 \text{ s}^{-1}$, $n = 7$) at [PTX] ≥ 100 nM, near the solution exchange rate. From measurements of reversal potential shifts upon exchanging the principal external cation, the permeability sequence for monovalent cations was: $\text{Cs}^+ \approx \text{K}^+ > \text{Na}^+ \gg \text{Tris}^+ > \text{tetramethylammonium}^+ > \text{TEA}^+ >$

$\text{NMDG}^+ \approx \text{tetrapropylammonium}^+ > \text{trimethylbutylammonium}^+ > \text{tetrabutylammonium}^+$. Ca^{2+} was also permeant ($P_{\text{Ca}} \approx P_{\text{NMDG}}$). Deactivation of the conductance on washout of PTX was extremely slow ($\tau_{\text{off}} > 300$ min) with internal and external Na^+ solutions, but relatively rapid ($\tau_{\text{off}} \approx 15$ min) with K^+ -containing solutions. Somewhat surprisingly, 50 nM PTX also induced the conductance, though with a 100-fold slower time course, in HEK293T cells during continuous incubation with 1 mM ouabain. In addition, in both HEK293T cells and guinea-pig ventricular myocytes, a 5-min preincubation with 0.5–1 mM strophanthidin, 1 mM dihydro-ouabain, or 1 mM ouabain, followed by exposure to 500 nM PTX in the absence of cardiotonic steroid, also markedly slowed activation of the conductance, yielding a τ_{on} sequence: control $<$ strophanthidin $<$ dihydro-ouabain $<$ ouabain. This suggests that activation of the PTX-induced conductance was limited by dissociation of the steroid because, in myocytes, the rate of recovery of Na/K pump current from inhibition by those steroids, after washing them out, showed the sequence strophanthidin $>$ dihydro-ouabain $>$ ouabain. Moreover, conductance activation by PTX on washout of steroid was faster than pump-current reactivation, in the same cell, on washout of the same steroid, suggesting that PTX can bind to a steroid-inhibited pump and accelerate dissociation of the steroid. This, in turn, implies that PTX and ouabain can simultaneously bind to the same Na/K pump. (Supported by NIH grant HL-36783.)

56. Activation of cAMP-dependent Protein Kinase A May Enhance Na/K Pump Current in Guinea-Pig Ventricular Myocytes CHIN OK LEE,* MASAYUKI SAKAGUCHI,* and DAVID C. GADSBY,[‡] **Pohang University of Science and Technology, Pohang, Korea; and [‡]The Rockefeller University, New York, New York 10021*

Na/K pump current was estimated as that abolished by 0.5 mM strophanthidin in myocytes superfused with modified Na-containing Tyrode's at $\sim 36^\circ\text{C}$ and internally dialyzed via pipettes perfused with solution including 50 mM Na^+ , 10 mM MgATP, and 50 or 100 nM Ca^{2+} . Steady membrane current at potentials between -100 and $+30$ mV was measured near the end of 40-ms steps from the 0-mV holding potential. The steady state Na/K pump current-voltage relationship was obtained by subtracting the I-V relationship determined in the presence of strophanthidin from the average of those determined, just before and just after, in its absence. As previously reported, Na/K pump current showed a variable tendency to run down (in a voltage-independent manner) with time after breaking into the cell. We examined the influence on the Na/K pump I-V curve of maximally stimulating PKA with forskolin (2–10 μM), monitored via the consistent, concomitant increase in CFTR Cl^- channel current: the effects on the Na/K pump were more variable, and a similar range of effects was seen at 50 and 100 nM pipette [Ca^{2+}]. Thus, in 5 of 28 myocytes examined, the Na/K pump I-V relationship seemed unaltered by either forskolin or the passage of time; whereas, in six other myocytes, Na/K pump current appeared little affected by forskolin, but similarly ran down in both its absence and presence. However, in nine other myocytes, Na/K pump current was reversibly increased (by $\sim 30\%$) by forskolin over the entire voltage range, and this stimulation was sometimes reproducible but often gradually declined with time after break-in. In seven further myocytes, the strophanthidin-sensitive current in forskolin seemed contaminated by a strophanthidin-induced increase in Cl^- conductance (likely reflecting stimulation of CFTR or swelling-activated Cl^- channels), precluding analysis

of forskolin action on the Na/K pump. In a final myocyte, examined using low-[Cl⁻] (sulfamate) Tyrode's to diminish such contaminating current, forskolin reversibly enhanced strophanthidin-sensitive current at all voltages. So it appears that PKA, stimulated by forskolin, can increase Na/K pump current, but that caution must be exercised in equating cardiotoxic steroid-sensitive current with that generated by the Na/K pump. (Supported by NIH grant HL36783.)

57. **NH₄⁺ Inhibits K-Cl Cotransport in Low K Sheep Red Blood Cells** PETER K. LAUF, SUHAIL AHMED, and NORMA C. ADRAGNA, *Departments of Physiology & Biophysics, and Pharmacology & Toxicology, Wright State University, Dayton, Ohio*

K-Cl cotransport (COT) is mediated by several isoforms of KCC proteins whose cDNAs have been recently cloned. We have earlier demonstrated that, in red blood cells (RBCs), K-Cl COT carries equally K⁺ and Rb⁺, as well as Cl⁻ and Br⁻. To further characterize the selectivity of the K⁺ site, we explored whether NH₄⁺ competes with K⁺ or Rb⁺ and is transported by K-Cl COT in low K (LK) sheep (S) RBCs before and after treatment with N-ethylmaleimide (NEM), a known stimulator of K-Cl COT (Lauf and Theg, 1980. *Biochem. Biophys. Res. Commun.* 92:1422). To minimize CO₂-driven Cl/HCO₃⁻ exchange facilitating intracellular NH₄Cl formation, and hence osmotic hemolysis, LK SRBCs were pretreated with the band-3 anion transport inhibitor DIDS in either Cl⁻ or SO₄²⁻ media. Both ouabain-resistant Rb⁺ influx and K⁺ efflux were measured in either NH₄Cl or (NH₄)₂SO₄, and Cl-dependent Rb/K fluxes (K-Cl COT) were calculated from the difference of the values in the two anions. NH₄⁺ (increased by replacing Na⁺) reduced basal and NEM-stimulated Cl-dependent Rb influx by mixed-type inhibition as both V_{max} decreased and K_m increased with rising NH₄⁺ concentrations. The K_i for NH₄⁺, estimated from Rb influx measurements, was ~50 mM and found to be three times larger than the K_m for Rb⁺ in these experiments, whereas the apparent K_i for NH₄⁺-inhibited Cl-dependent K⁺ efflux was 45 mM. Experiments taking advantage of an external acid pH-induced conversion of NH₃ to NH₄⁺ were inconclusive: NEM per se modified the pH response of K-Cl COT. To test whether NH₄⁺ is actually transported by the K-Cl COT system, Cl-dependent hemolysis was measured in the presence and absence of calyculin and genistein, inhibitors of protein phosphatases and kinases, respectively, and of K-Cl COT. However, no indirect evidence for NH₄⁺ transport by the system could be detected with this method. The flux data suggest that in DIDS-treated LK SRBCs, NH₄⁺ binds to an external low-affinity site in the transporter and causes allosteric inhibition of K-Cl COT. These results are consistent with the lack of NH₄⁺ transport by the hemolysis approach.

58. **Cation-Anion-coupled Cotransport in an Immortalized Neuronal Cell Line (C6 Glioma)** KENNETH B.E. GAGNON,* NORMA C. ADRAGNA,† ROBERT E.W. FYFFE,§ and PETER K. LAUF,* **Department of Physiology and Biophysics, †Department of Pharmacology and Toxicology, §Department of Anatomy, and ¶Department of Brain Research Center, Wright State University, Dayton, Ohio*

Ion gradients across the cell membrane are vitally important for proper cell-to-cell communication and general cell homeostasis and are maintained by both primary (ATP-dependent) and

secondary active transport mechanisms. Among the latter, Na-K-2Cl cotransport (COT) is present in primary cultures of rat astrocytes (Tas et al. 1987. *Biochim. Biophys. Acta.* 903:411-416) and implicated in the K spatial buffering capacity of glial cells. However, no reports on the presence of glial K-Cl COT are available yet. The present work was designed to study Na-K-2Cl COT and K-Cl COT in C6 glioma cells. Cell cultures were grown to confluence under 5% CO₂ supplemented air atmosphere in 12-well plates using F12K essential medium containing 15% horse serum, 2.5% fetal bovine serum, and penicillin/streptomycin. Influx of Rb (a K congener) was measured under initial velocity conditions at 6 min and 37°C in Na media containing (mM): 10 RbCl, 2 CaCl₂, 1 MgCl₂, 10 glucose, buffered to pH 7.4 with 20 HEPES/TRIS. Rb influx (nmol/mg protein × min) was 16.0 in the absence of inhibitors, 14.3 with 1.0 mM ouabain, 7.9 with ouabain and 0.005 mM bumetanide, and 4.3 with the additional presence of 2 mM furosemide. Thus, the Na/K pump represents 10% of the total Rb influx, whereas the Na-K-2Cl COT and K-Cl COT represent 40 and 22%, respectively. Na-K-2Cl COT was inhibited in a dose-dependent manner by bumetanide, whereas 100% inhibition of K-Cl COT occurred at 2 mM furosemide. At its maximum effective concentration, NEM stimulated the Na/K pump and K-Cl COT by 2- and 10-fold, respectively, and inhibited Na-K-2Cl COT by 100%. Cell K contents remained relatively unchanged, but fell by ~20% after NEM treatment, suggesting opening of a K channel, reported by us in other cells. Using a polyclonal anti-rabbit KCC1 antibody (generously supplied by Dr. Eric Delpire), K-Cl COT in C6 glioma cells was immunohistochemically demonstrated by a strong, punctuate immunofluorescent labeling throughout the cytoplasm and cell membrane. Our results on cultured C6 glioma cells corroborate the immunological findings of Plotkin et al. (1997. *Am. J. Physiol. Cell Physiol.* 272:C173-C183) and the RT-PCR results of Payne et al. (1996. *J. Biol. Chem.* 271:16245-16252) showing the KCC1 isoform in astrocytes. Western blots using the same anti-rabbit KCC1 antibody revealed a single strong band of ~120 kD, presumably the cytosolic, unglycosylated K-Cl cotransporter. These studies have therefore established: (a) the functional presence of the Na/K pump, and both Na-K-2Cl and K-Cl COT; (b) the immunohistochemical presence in C6 glioma cells of a KCC isoform of K-Cl COT; and (c) inactivation of Na-K-2Cl COT and simultaneous stimulation of K-Cl COT by NEM, possibly implicating a shared regulatory pathway. Studies in progress are aimed at the Cl dependence and the critical NEM concentration inversely affecting Na-K-2Cl and K-Cl COT. (Supported in part by NIH, AHA, and a WSU SOM alpha grant.)

59. **Transient Nature of the Stimulatory "NEM-Effect" on K-Cl Cotransport in KCC1-transfected HEK293 and Primary Rat Aortic Smooth Muscle Cells** PETER K. LAUF,* JIN ZHANG, JING ZHANG, and NORMA C. ADRAGNA,† **Department of Physiology and Biophysics, and †Department of Pharmacology and Toxicology, Wright State University, Dayton, Ohio*

K-Cl cotransport (COT) is mediated by several isoforms of KCC proteins whose cDNAs have been recently cloned. The thiol reagent N-ethylmaleimide (NEM) (Lauf and Theg, 1980. *Biochem. Biophys. Res. Commun.* 92:1492) has been widely used to demonstrate, by several-fold stimulation, the presence of K-Cl COT in a variety of cells such as red blood cells (RBCs), rat aortic smooth muscle cells (RASMCs), and human embryonic kidney (HEK293) cells transfected with KCC isoforms. In RBCs, NEM

was proposed to inhibit a kinase that by phosphorylation inactivates K-Cl COT (Jennings and Al Rohil. 1999. *J. Gen. Physiol.* 114:743). Contrary to our work with RBCs, where the "NEM effect" is stable over time, we report here on the transitory nature of this NEM effect in HEK293 cells and primary RASMCs. HEK293 cells either not transfected (normal) or transiently transfected with full-length rbKCC1cDNA (kindly provided by Drs. Gillen and Forbush, Yale University) and RASMCs were treated with NEM concentrations yielding maximum stimulation of endogenous or transfected K-Cl COT. The activity of the system was tested by Rb influx, at various times within 1 h of NEM treatment and removal by washing, in Cl or sulfamate media containing (mM) 0.1 ouabain, 0.01 bumetanide, and 0.01 GdCl₃ to inhibit the Na/K pump, Na-K-2Cl COT, and stretch-activated K channels. K-Cl COT is the calculated difference between Rb influx in Cl and sulfamate. Treatment with NEM for 10 min stimulated K-Cl COT by threefold in normal and eightfold in KCC1-transfected cells, and by fivefold in RASMC. The NEM effect was abolished in normal HEK293 cells, and fell by 80% in rKCC1-transfected cells and RASMC after 45 and 10 min, respectively. Full K-Cl COT stimulation was observed in HEK293 cells incubated for 45 min before 10-min NEM treatment and subsequent flux. Furthermore, HEK293 cells first treated with NEM, and then washed and again exposed to NEM, also lost the stimulation of K-Cl COT. Dithiothreitol, a reducing agent, failed to preserve the NEM effect. It is known that the NEM-effect requires the presence of ATP (Lauf. 1983. *Am. J. Physiol. Cell Physiol.* 245:C445). There was no significant difference in the ATP content of control and NEM-treated cells. In contrast, cellular GSH fell by 90%, suggesting a breakdown of the cellular redox potential rather than NEM action through inhibitory thiols as in RBCs (Lauf and Adragna. 1995. *Am. J. Physiol. Cell Physiol.* 269:C1167). We suspect that, in both HEK293 cells and RASMC, NEM induced the initial dephosphorylation responsible for K-Cl COT stimulation, followed by changes in the transport complex resulting in the complete and irreversible dissipation of the stimulatory "NEM effect." (Supported in part by an AHA grant.)

60. Effect of Media pH on the Kinetics of the Sodium/Bicarbonate Cotransporter (NBC) RONA G. GIFFARD and RONALD L. MORGAN, *Department of Anesthesia, Stanford University, Stanford, California*

Regulation of pH in the brain is critical to normal physiological function and in response to pathophysiological disturbances such as cerebral ischemia. NBC is localized to glial cells in the brain. This transporter is DIDS inhibitable, bicarbonate dependent, and electrogenic. When running in an inward direction, NBC alkalizes the cell. The associated extracellular acidification can dampen neuronal excitability (Rose and Ransom. 1996. *J. Physiol.* 491:291–305). In this study, the effects of acidification on the kinetics of NBC activity of primary cultured astrocytes from mouse cortex were determined. Sodium uptake using ²²Na⁺ was used to determine the kinetics of astrocyte NBC.

Astrocyte cultures, prepared from cortices of neonatal Swiss Webster mice, were used after 20–30 d in vitro. Cultures were washed with buffered saline solution containing 5.5 mM glucose (BSS 5.5) at pH 7.4 or 6.8 in the absence of HCO₃⁻. After the last wash, the cells were preincubated for 1 h at 37°C in the same buffer. At the end of the preincubation period, the buffer was removed from each well and BSS 5.5 buffer with HCO₃⁻ was added. This buffer contained 1 mM ouabain, to inhibit the Na⁺/K⁺ ATPase, 10 μM 5-(N-methyl-N-isobutyl) amiloride to inhibit

Na⁺/H⁺ exchange and sodium (35–147 mM). The bicarbonate concentrations in the BSS 5.5 buffers at pH 6.8 and 7.4 were 6 and 26 mM, respectively. After adding the BSS 5.5 buffer, 0.2 μCi of ²²Na⁺ was added to each well and incubated for 2–6 min. Then the cells were washed with ice-cold phosphate-buffered saline and solubilized with 2% SDS. Aliquots were taken for gamma counting. Initial transport velocities were determined from the time versus sodium uptake plots. The initial velocities and the sodium concentrations were then plotted on a dual reciprocal plot for each pH value.

At a pH value of 7.4, the dual reciprocal plot was a straight line, while at a pH value of 6.8, nonlinear inhibition was found. This type of inhibition indicates that either more than one form of the transporter is present, and the different forms respond differently to acidosis, or that the transporter may associate into a multimeric form or be modified, such as by phosphorylation, in response to the pH. To begin to analyze these different possibilities, the cloned brain NBC (Giffard et al. 2000. *J. Neurosci.* 20:1001–1008) is being expressed in 3T3 cells that do not normally show significant NBC-like activity. This will permit characterization of the behavior of a single species of NBC as a function of pH.

61. Transport Mechanism of the Organic Cation Transporter 2 THOMAS BUDIMAN, ERNST BAMBERG, HERMANN KOEPEL, and GEORG NAGEL, *Max-Planck-Institut für Biophysik, D-60596 Frankfurt, Germany*

The organic cation transporter 2 (OCT2) is expressed in kidney and brain, where it serves in homeostasis of exogenous and endogenous amines. We expressed rat OCT2 in *Xenopus laevis* oocytes and studied substrate-induced changes of electrical current with the giant patch-clamp technique. Activation of electric current corresponding to efflux was observed for small organic cations; e.g., tetramethylammonium (TMA), choline, and tetraethylammonium (TEA). In contrast, the bigger cations quinine and tetrabutylammonium (TBA) elicited no change in patch current. However, transport of TMA, choline, and TEA could be inhibited by applying quinine or TBA to the cytoplasmic side. We show that inhibition of organic cation efflux by quinine was competitive with substrates, with an apparent affinity constant of ~1 μM. Transport-mediated electrical current was linearly voltage dependent, with maximal turnover and apparent affinity to substrates both showing voltage dependence. Inclusion of organic cations in the pipette (i.e., the outside) revealed organic cation-induced inward current. Organic-cation-induced currents in both directions were observed when substrates were present on both sides of the membrane. At saturating concentrations of substrates, the resulting conductance was substantially smaller than at transzero conditions. Our results exclude an electroneutral H⁺/organic cation⁺ exchange and suggest the existence of an electroneutral organic cation⁺/organic cation⁺ exchange. We propose a model for a carrier-type transport mechanism. (Supported by DFG and MPG.)

62. Pre-Steady State Kinetics of the Neuronal Glutamate Transporter EAAC1 NATALIE WATZKE,* MICHAEL WIESSNER,† THOMAS RAUEN,‡ and CHRISTOF GREWER,* **Max-Planck-Institut für Biophysik, Frankfurt, Germany; and †Max-Planck-Institut für Hirnforschung, Frankfurt, Germany (Sponsor: Georg Nagel)*

Glutamate transporters are important for the rapid removal of glutamate from the synapse after excitatory neurotransmission. We have demonstrated the use of glutamate concentration jumps initiated by laser-pulse of caged glutamate together with current recording from voltage-clamped excitatory amino acid carrier 1 (EAAC1)-expressing cells for the investigation of rapid glutamate transporter reaction steps with a 100- μ s time resolution. Here, we used this method to study the Na⁺/glutamate translocation step in the transport cycle in detail. In the forward transport mode of EAAC1, this reaction is accelerated by negative transmembrane potentials and takes place with a time constant of 7–8 ms at 0 mV. The reaction is also observed when the transporter is studied under Na⁺/glutamate-homoechange conditions (substrates present on both sides of the membrane). However, when only Na⁺, but not glutamate, is present on the intracellular side of the membrane, we observe an additional voltage-dependent process with a time constant of \sim 40 ms. Interestingly, the same effect is obtained when intracellular Na⁺ is replaced by Li⁺. The results are consistent with a model in which Na⁺/glutamate translocation across the membrane is followed by a Na⁺-dissociation step that leads to the release of at least one Na⁺ ion into the cytoplasm before glutamate dissociation takes place. (Supported by the DFG and the MPG.)

63. Knockout Mouse Red Cells Expressing Human HbC or HbS and γ Have High K:Cl Cotransport Activity in Contrast to HbA Mouse Red Cells JOSE R. ROMERO,* SANDRA M. SUZUKA,[†] GRACE V. ROMERO-GONZALEZ,* RONALD L. NAGEL,[†] MARY E. FABRY,[†] *Endocrine-Hypertension Division, Brigham and Women's Hospital, Harvard Medical School, Boston, Massachusetts; and [†]Division of Hematology, Albert Einstein College of Medicine, Montefiore Medical Center, Bronx, New York

K:Cl cotransport (KCl) is elevated in humans with homozygous HbS (SS) or homozygous hemoglobin C (CC). In the case of SS, at least part of this elevation is correlated with increased reticulocyte count since density fractions rich in retics have higher KCl activity. The case for HbC disease is less clear, since KCl in CC red cells is nearly as high as SS red cells, but retic counts are lower. KCl in early transgenic mice expressing human α and β^S or β^{SAD} and residual mouse globins is further complicated by the fact that NO₃⁻, which inhibits KCl in all other mammalian systems, not only does not inhibit transport, but stimulates it. Dihydroindenyl-oxy-alkanoic acid (DIOA) also inhibits KCl in most mammalian systems, but is not effective in mouse red cells expressing human α and β^S or β^{SAD} and residual mouse globins.

We report on KCl in three lines of knockout (KO) mice expressing exclusively human hemoglobins: mice with HbA, HbC, and HbS+37% γ . We find that HbA mice have a small volume of stimulated KCl (2.6 \pm 0.3 mmol/liter cell per h [FU] vs. sulfamate) that is stimulated by NO₃⁻, as reported in previous studies of early transgenic lines. In KO mice expressing exclusively human HbC or HbS+ γ , the results are very different: KCl had a strong volume-stimulated component (9.8 \pm 0.5 and 10.1 \pm 1.1 FU for C and S+ γ mouse red cells vs. sulfamate, respectively) that was partially inhibited by NO₃⁻ (48 vs. 37% for C and S+ γ mouse red cells, respectively) and also by DIOA (41 vs. 28% for C and S+ γ mouse red cells, respectively). A similar but more pronounced effect was observed for KCl activity measured at pH 7.0, which was even more pronounced for HbC mice.

We have also studied K:Cl cotransport in the founder mice expressing 56% human α and 33% β^C and residual mouse globins. We found a strong volume dependence (8.6 \pm 0.6 FU vs. sulfamate) and sensitivity to NO₃⁻ (34%) and DIOA (30%) in these mice as well. This is in contrast to the findings with transgenic mice expressing \sim 56% human α and 75% β^S and residual mouse globins. We therefore conclude that β^C interacts differently and more strongly with the transporter and/or its regulators than does β^S .

In summary, we find that the presence of HbC and HbS+ γ , in the absence of mouse globins, have both a significant quantitative and a qualitative effect on KCl in mouse red cells. We conclude that both mouse and human globins are able to affect activity and/or regulation of KCl in mouse red cells. Also, the K⁺ transport detected by sulfamate may represent the contributions from two different transporters: KCl and a second, yet to be defined, transporter particularly active in murine red cells. (Supported by NIH grant P60HL38655, Bronx Comprehensive Sickle Cell Center.)

64. Cation Selectivity and Coupling by SGLT Cotransporters Is Modulated by a Conserved Acidic Amino Acid Residue MATTHIAS QUICK and ERNEST M. WRIGHT, Department of Physiology, School of Medicine, University of California Los Angeles, Los Angeles, California

The human Na⁺/glucose cotransporter (hSGLT1) is the archetype of a large family of symporters encompassing homologs from archaea, bacteria, yeast, insects, and mammals (Turk and Wright. 1997. *J. Membr. Biol.* 159:1–20). These integral membrane proteins use the electrochemical Na⁺ gradient to drive the uphill transport of a variety of substrates into cells. For hSGLT1, it was shown that the sugar pathway is located in the COOH-terminal domain of the protein and that conformational changes couple Na⁺/glucose cotransport (Wright et al. 1996. *Curr. Opin. Cell Biol.* 8:468–473). Evidence for the role of the NH₂-terminal domain in cation binding/translocation comes from another member of the SGLT-family (PutP; Quick et al. 1999. *Biochemistry.* 38:13523–13529). Here we describe the effects of replacing Asp204 in hSGLT1 located in a short cytoplasmic loop of the transporter that is conserved within the prokaryotic and eukaryotic members of the SGLT family. Glu in place of Asp204 increases the apparent affinity for H⁺ by more than one order of magnitude with only a little impact on the apparent Na⁺ affinity. Removal of the negative charge (Asp204 \square Asn or Cys) reduces the number of transporters in the plasma membrane approximately fivefold. The pattern of the kinetic parameters of the D204C and D204N transporter is similar and shows a >10-fold increase of the apparent Na⁺ affinity. Although the apparent affinity of these transporters for H⁺ has not changed, the turnover rates of H⁺/glucose cotransport are increased >>10-fold. While the stoichiometry of cation/glucose cotransport for hSGLT1 is 2 Na⁺ (or H⁺):1 glucose, the coupling ratio for the D204N transporter is 33 H⁺:1 glucose, but there is no change on the Na⁺/glucose stoichiometry. These results show that the conserved Asp204 in hSGLT1 is critical for cation selectivity and coupling of cation/substrate cotransport. Together with information from other members of the SGLT family, it is proposed that this region is involved in coupling cation and substrate transport, and that the binding sites for the cosubstrates may be in close proximity. (Supported by NIH grant DK19567 to E.M. Wright. M. Quick was a fellow of the Deutsche Forschungsgemeinschaft.)

65. Identification of Sites of Intermolecular Crosslinking in the Erythrocyte Band 3 Protein HIROYUKI KUMA, ANJALI SHINDE, TODD HOWREN, and MICHAEL L. JENNINGS, *Department of Physiology and Biophysics, University of Arkansas for Medical Sciences, Little Rock, Arkansas*

The erythrocyte anion exchange protein (band 3 or AE1) is a homodimer of 95-kD subunits; the dimers can associate further into tetramers. The membrane-impermeant bifunctional reagent bis(sulfosuccinimidyl) suberate (BS³) is known to crosslink human band 3 to a covalent dimer in intact cells (Staros. 1982. *Biochemistry*. 21:3950–3955). The purpose of this study was to identify lysine residues that participate in the intermolecular crosslink. To determine whether the covalent crosslink is between subunits of the tightly associated band 3 dimer or between two different dimers in a tetramer, high performance gel filtration (TSK G4000SW) in nondenaturing detergent was performed on band 3 from control and BS³-treated cells. The proportions of dimer and tetramer are not changed by BS³ treatment, indicating that the crosslink is between subunits of the dimer and not between different dimers in a tetramer. To identify crosslinked residues, two approaches were used: proteolytic cleavage of the native protein and site-directed mutagenesis of the protein expressed in HEK293 cells. For the proteolysis experiments, cells were first treated with H₂DIDS (4,4'-diisothiocyanatodihydrostilbene-2,2'-disulfonate) to form an intramolecular crosslink between K539 and K851; this crosslink does not interfere with the BS³ intermolecular crosslink. Cells were then treated with radiolabeled BS³, followed by chymotrypsin, and then papain. Chymotrypsin excises a small peptide (N554-L558) without disrupting the BS³ crosslink. Papain cleaves at Q550 and Q564 and causes the protein to run on gels as a monomer (still internally crosslinked with H₂DIDS). A crosslinked peptide was isolated from the supernatant after papain digestion; results of Edman degradation were exactly as expected if the peptide were K551-Y553 crosslinked to M559-Q564. This indicates that K551 on one subunit can be crosslinked to K562 on the other subunit. To investigate further the role of these lysine residues in the intermolecular crosslink, the AE1 membrane domain was expressed in HEK293, using the Ecdysone system. The protein traffics to the plasma membrane and can be crosslinked to a dimer by BS³ in intact HEK293 cells. With point mutations K551Q or K562Q, the membrane domain is still expressed on the plasma membrane, but is not crosslinked by BS³; this finding is additional evidence that K551 and K562 participate in the crosslink. The identification of K551 and K562 as sites of intermolecular crosslinking places significant restrictions on the possible arrangements of the AE1 polypeptide in the dimer. (Supported by NIH grant R01 GM 26861.)

66. Multilevel Regulation of the Human Nucleoside Transporters IMOGEN R. COE, MICHA PENNY-COOKE, NAZ CHAUDARY, DIMITRA TZAMTZIS, and IRINA SHURALYOVA, *Department of Biology, York University, Toronto, Ontario, Canada* (Sponsor: Amira Klip)

Nucleoside transporters are responsible for the movement of nucleosides such as adenosine and nucleoside analog drugs across cell membranes. The human equilibrative nucleoside transporter, hENT1, is the mostly widely distributed nucleoside transporter in human tissue. However, expression levels vary considerably between tissues. Very high levels of expression in endocrine and cardiovascular tissue suggest tissue-specific transcriptional regulatory mechanisms. In addition, there are striking dif-

ferences in expression levels between individuals and between normal and transformed tissue for all nucleoside transporters. Quantitative analysis of difference expression levels provides insight into transcriptional regulation of nucleoside transporters. In addition, analysis of the promoter region of the hENT1 gene suggests regulatory factors that control expression.

Our research also suggests that additional levels of regulation of nucleoside transporters may exist. Manipulation of protein kinase C (PKC) pathways can strongly influence acute uptake of nucleoside via hENT1 in MCF-7 and HeLa cells, suggesting post-translational regulation. The PKC isoforms responsible for the effects have been identified. Use of recombinant tagged transporters and mass spectroscopic analysis will help to elucidate the underlying mechanisms involved in this regulation. Multilevel regulation of nucleoside transporters suggests different cellular mechanisms exist to ensure homeostatic levels of nucleosides are maintained. The ability to manipulate transporter activity may have therapeutic applications in the development of improved uptake of analog drugs. (Supported by NSERC, MRC and NCIC.)

67. Towards a Definition of the Permeation Pathway in the Serotonin Transporter: Importance of the First Transmembrane Domain ERIKA M. ADKINS and RANDY D. BLAKELY, *Department of Pharmacology and Center for Molecular Neuroscience, Vanderbilt University School of Medicine, Nashville, Tennessee* (Sponsor: Kevin Strange)

The cocaine and antidepressant-sensitive serotonin (5-hydroxytryptamine, 5-HT) transporter (SERT) is a putative 12-transmembrane domain (TMD) protein critical for the termination of 5-HT signaling in the CNS and the periphery. However, neither the SERT residues comprising a permeation pathway, nor those functional groups on 5-HT contacting these residues is known. Previous studies in our laboratory have determined the sites of interaction of SERT antagonists using SERT chimeras and species-scanning mutagenesis and the divergent pharmacologic properties of human and *Drosophila* SERTs (hSERT and dSERT, respectively). We have adopted these methods to search for domains and residues controlling the permeation of 5-HT itself. Screening of tryptamine derivatives against hSERT and dSERT reveals rank order potency differences for the blockade of [³H]-5-HT uptake in the two species variants with differences in potency up to 40-fold evident. Using cross-species chimeras and species-scanning mutagenesis, we have established that TMD I, specifically an aromatic residue (Y95 in hSERT, F90 in dSERT), contributes to the ability of derivatives with bulky indole nitrogen constituents and seven-position substitutions to discriminate hSERT and dSERT. Interestingly, this TMD I aromatic amino acid was previously implicated by our lab in antagonist recognition, and a D residue one putative helix turn away from this aromatic residue implicated in 5-HT interaction. These and other findings have led us to investigate the possibility of TMD I functioning as a structural motif in a permeation pathway for 5-HT and cosubstrates. To test this hypothesis, we mutated individual residues in TMD I of hSERT to cysteine to examine accessibility to methanethiosulfonate (MTS) derivatives. In general, cysteine mutants from the extracellular-facing half of the putative helix exhibit reactivity at concentrations as low as 0.01 mM MTSET and as early as 30 s, while mutants on the internal face of the membrane possess little or no reactivity to MTS reagents. Within the upper half of the putative helix, a periodic pattern of accessibility is observed that suggests an alpha-helical conformation. Furthermore, studies examining the effects of 5-HT on the accessibility of MTS reagents

show that, in the presence of a transported ligand, the extracellular half of the TMD becomes less reactive towards MTSET, while the intracellular half becomes more reactive, suggesting movement of the TMD upon binding and/or translocation of 5-HT. Ongoing studies are evaluating the ability of antagonists to protect against or enhance MTS-induced inactivation, and also examining the utility of biotinylated MTS reagents to probe the depth and selectivity of reagent accessibility. (Supported by NIH grants MH12399 to E.M. Adkins and DA07390 to R.D. Blakely.)

68. Active Transport of Potassium and the Structures of the TRK Proteins in the Yeast, *Saccharomyces cerevisiae* CLIFFORD L. SLAYMAN,* ADAM BERTL,† HERMANN BIHLER,*† STEWART R. DURELL,§ and H. ROBERT GUY,§ *Cellular and Molecular Physiology, Yale School of Medicine, New Haven, Connecticut; †Botanisches Institut I, Universität Karlsruhe, Germany; and §Laboratory of Experimental and Computational Biology, National Cancer Institute, Bethesda, Maryland

Background. Energy-dependent uptake of K^+ by *Saccharomyces cerevisiae* is mediated by at least three systems, which have high, medium, and low affinity for K^+ , where the terms relate to Michaelis constants of $\sim 10 \mu\text{M}$, $\sim 3 \text{ mM}$, and $\sim 50 \text{ mM}$. The high- and medium-affinity systems involve two related genes/proteins, TRK1 and TRK2 (Gaber et al. 1986. *Mol. Cell. Biol.* 8:2848; Ko and Gaber. 1991. *Mol. Cell. Biol.* 11:4266). The low-affinity system(s) is not yet identified, and may represent facultative behavior of transporters with other primary functions. A reasonable guess about their modes of operation—extrapolated from earlier information on *Neurospora* (Rodriguez-Navarro et al. 1986. *J. Gen. Physiol.* 87:649)—is that Trk1p couples the uptake of each K^+ to the coflux of one proton, but that Trk2p does that poorly if at all.

New results. Details of K^+ flux in *Saccharomyces* have become very complicated, and suggest both that Trk1p and Trk2p may be components of a larger complex, and that Trk2p normally carries a substantial non- K^+ current. Sequence analysis of the dozen known TRK-type proteins has identified them with three bacterial protein families (i.e., TrkH,G in *E. coli*, KtrB in *V. alginolyticus*, and the KcsA channel of *S. lividans*). Starting with this sequence analysis and the known crystal structure of KcsA (Doyle et al. 1998. *Science*. 280:69), Durell and Guy (1999. *Biophys. J.* 77:785) have drawn atomic-scale models of all three families, leading to clear-cut predictions about structure–function relationships and the transport mechanism. The broad similarities of Trk1,2p to bacterial K^+ transporters, which are known to function in hetero-oligomers, also suggests specific types of interacting proteins to search for in *Saccharomyces*.

69. Normal and Sick Erythrocytes Have Different K-Cl Cotransport Inactivation Profiles in Aging Cells: This Is Not Accompanied by Differences in Membrane-associated Protein Phosphatase-1 ISABEL BIZE, SAMARA TAHER, and CARLO BRUGNARA, Department of Pathology, Children's Hospital, Harvard Medical School, Boston, Massachusetts

The activity of K-Cl cotransport (KCC) is elevated in young normal erythrocytes (AA cells) and in erythrocytes with hemoglobin SS (SS cells, sickle cells) compared with the activity in mature AA cells. In AA and SS cells, the activity of KCC in isotonic condi-

tions (basal KCC) decreases as cell density increases, a reflection of cell maturation and aging. In AA cells, the progressive decrease in KCC activity is associated with a progressive decrease in membrane-associated protein phosphatase-1 (mb-PP1) activity, an activator of KCC. We tested the hypothesis that the elevated activity of KCC in SS cells is secondary to elevated mb-PP1 activity. We determined basal KCC and mb-PP1 activity in fractions of AA and SS cells separated in isotonic discontinuous density gradients. KCC activity was determined using Cl-dependent ^{86}Rb influx in isotonic conditions. Mb-PP1 activity was determined using ^{32}P -labeled phosphorylase-a as substrate, and membranes obtained from cells were lysed in isotonic conditions. Our results show that in the least dense AA and SS cells [mean cell density (CHCM) $\sim 25 \text{ g/dl}$ hemoglobin (Hb)], KCC activity and mb-PP1 activity are identical in both types of cells; in AA cells, KCC activity is $0.30 \pm 0.08 \text{ mmol/liter cells} \cdot \text{h}$ ($n = 6$), and mb-PP1 activity is $0.76 \pm 0.10 \text{ U/mg membrane protein}$ ($n = 17$). In SS cells, KCC activity is $0.26 \pm 0.08 \text{ mmol/liter cells} \cdot \text{h}$ ($n = 6$), and mb-PP1 activity is $0.68 \pm 0.13 \text{ U/mg membrane protein}$ ($n = 4$). However, in AA cells, KCC activity decreases as a steep function of increasing cell density (at CHCM $\sim 27 \text{ g/dl}$, Hb activity is 23% of activity at $\sim 25 \text{ g/dl}$ Hb), and this decrease is paralleled by a more gradual decrease in mb-PP1 activity (at CHCM $\sim 27 \text{ g/dl}$, Hb activity is 60% of activity at $\sim 25 \text{ g/dl}$ Hb). In contrast to AA cells, KCC in SS cells is fully active at $\sim 30 \text{ g/dl}$ Hb, while mb-PP1 activity is identical in AA and SS cells at all cell densities. KCC is almost completely inactivated at 32 and 34 g/dl Hb in AA and SS cells, respectively. The CHCM at which KCC is half maximal (CHCM_{50,KCC}) is ~ 26 and $\sim 31 \text{ g/dl}$ Hb in AA and SS cells, respectively. The results indicate that the increased KCC activity of SS cells is attributable not to an initially elevated KCC activity in least-dense (young) SS cells, nor to an inability of SS cells to inactivate the transporter, but rather to a shift in the CHCM_{50,KCC}, suggesting that SS cells have a slower decay in KCC activity during cell maturation and aging. The shift in CHCM_{50,KCC} in SS cells is not accompanied by a similar shift in the CHCM_{50,mb-PP1}. Rather, the differences in the CHCM_{50,KCC} in AA and SS cells must be secondary to differences in other regulators, or to an impairment in transporter processing. (Supported by NIH grants HL-15157 and DK-50422.)

70. The Permeability of Fructose-1,6-Diphosphate in Cardiomyocytes BENJAMIN CHIANG,* SUFAN CHIEN,* LIYIN CHI,* OULI WANG,† and WILLIAM EHRINGER,† *Jewish Hospital Heart and Lung Center, Cardiothoracic Surgical Research Institute, Department of Surgery; and †Center for Applied Microcirculation Research, University of Louisville School of Medicine, Louisville, Kentucky (Sponsor: Nichilas A. Delemere)

FDP has been used to protect various organs against ischemic and reperfusion injuries. The ability of FDP to cross the cell membrane and be metabolized remains controversial. The aim of this study was to test the hypothesis that FDP would cross the cardiomyocyte membrane under normoxia and hypoxia.

Adult rat cardiomyocytes were harvested and suspended in culture media with FDP and spiked with $0.1 \mu\text{Ci } ^{14}\text{C-FDP}$. The cells were incubated at 37°C under normoxia (5% CO_2 and room air) and hypoxia (5% CO_2 and 95% N_2) for 1 and 16 h. The culture media with cardiomyocytes were centrifuged. The supernatants were saved for liquid scintillation, and the cardiomyocyte pellets were washed with HBSS. The radioactivity of supernatants and cells was measured by liquid scintillation counter. The uptake of

FDP was expressed as the partition coefficient of FDP in cells. The cells with culture media incubated under normoxia or hypoxia also were incubated with alamar blue for evaluation of the viability of the cells.

The partition coefficients of FDP in cardiomyocytes were increased under normoxia or hypoxia in a concentration-dependent manner. At 16 h incubation under normoxia, the partition coefficient in 50 mM of FDP was $6.62 \pm 0.07\%$, higher than those in 0, 5, 10, and 25 mM, but under hypoxia the highest partition coefficient was in 25 mM FDP. (Fig. 2). The partition coefficients of FDP in cardiomyocytes were higher under hypoxia than under normoxia (Fig. 2). The viability of cardiomyocytes indicated by relative fluorescence of alamar blue revealed a similar tendency (Fig. 3).

Our previous studies demonstrated that FDP can passively diffuse through egg phosphatidylcholine membrane bilayers and may disrupt membrane permeability and swell the vesicles (Ehringer et al. 2000. *Mol. Cell. Biochem.* In press), and FDP improves hypothermic rat heart preservation. (Chien et al. 2000. *J. Heart Lung Transplant.* 19:277–285). Our present study demon-

strates that the uptake of FDP by cardiomyocytes follows a concentration-dependent type response under either normoxia or hypoxia. The uptake of FDP by cardiomyocytes seems to be increased under hypoxia compared with normoxia. This finding, if further confirmed, will have significant therapeutic importance, because this is the situation where enhanced glycolytic energy production is needed.

This study appears to demonstrate that FDP could cross the cardiomyocyte membrane and that the uptake of FDP by the cells increases under hypoxia and the permeability increases as the concentration of FDP is increased. (Supported in part by American Heart Association, Ohio affiliated, grant 9807757, and a grant from the Jewish Hospital Foundation.)

Partition Coefficient of ^{14}C -FDP in Cardiomyocytes (16 hrs + 1 hr reoxygenation)

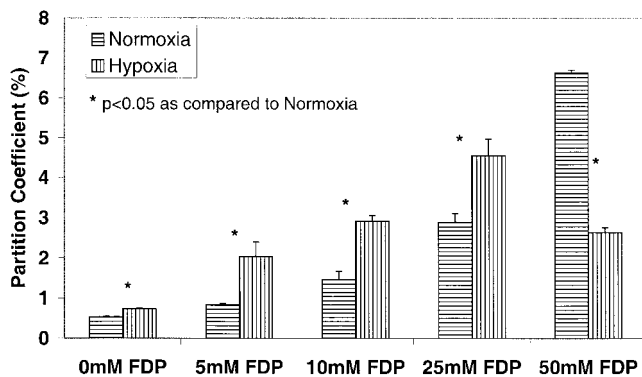


FIGURE 2.

Relative Fluorescence in Cardiomyocytes (16 hrs + 1 hr Reoxygenation)

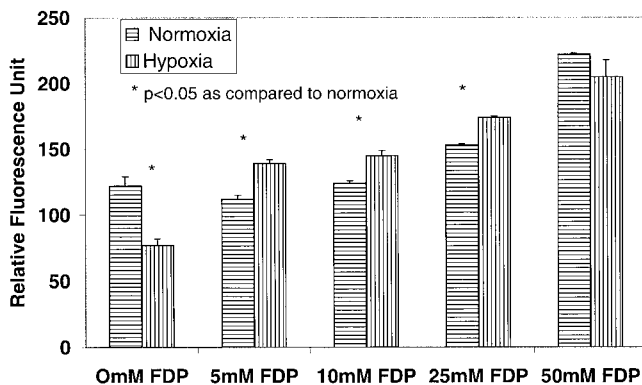


FIGURE 3.

71. Which Voltage-gated Proton Channels Are Activated by PMA during the Respiratory Burst in Human Neutrophils? VLADIMIR V. CHERNY,* LARRY L. THOMAS,[†] and THOMAS E. DECOURSEY,* *Department of Molecular Biophysics and Physiology, and [†]Department of Immunology/Microbiology, Rush Presbyterian St. Luke's Medical Center, Chicago, Illinois

Generation of reactive oxygen species by the NADPH oxidase complex is a major bactericidal weapon of phagocytes. Phorbol myristate acetate (PMA) is a potent agonist for this "respiratory burst" in human neutrophils. Although H^+ efflux occurs during the respiratory burst, efforts to stimulate voltage-gated H^+ channels with PMA in whole-cell, patch-clamped phagocytes have been unsuccessful. We have employed a modification of the permeabilized-patch configuration that allows control of pH_i and preserves second messenger pathways. Using this method, we show that PMA dramatically enhances and alters voltage-gated proton currents in human neutrophils (DeCoursey et al. 2000. *Proc. Natl. Acad. Sci. USA.* In press). PMA produces four alterations in H^+ current properties, each of which increases the H^+ current at a given voltage: (a) a 40-mV negative shift in the $g_{\text{H}}\text{-V}$ relationship, (b) faster activation (smaller τ_{act}) during depolarizing pulses, (c) slower deactivation (larger τ_{tail}) upon repolarization, and (d) a larger maximum H^+ conductance, $g_{\text{H,max}}$. The induced g_{H} had properties identical with a "novel" proton conductance described recently in human eosinophils (Bánfi et al. 1999. *J. Exp. Med.* 190:183–194). This g_{H} activates at more negative voltages than the "normal" g_{H} , and thus allows inward H^+ current. A non-voltage-gated inward current that directly reflects electron transport by NADPH oxidase was also activated by PMA. The identity of this electron current was confirmed by its sensitivity to diphenylene iodinium (DPI), an inhibitor of NADPH oxidase. DPI did not alter the increased $g_{\text{H,max}}$ or the faster τ_{act} in PMA-stimulated neutrophils, but did reverse the slowing of τ_{tail} with a time course paralleling its inhibition of electron current. A complex interaction between NADPH oxidase and voltage-gated proton channels is indicated. The amplitudes of H^+ and electron currents activated by PMA were not correlated. Thus, it is unlikely that the H^+ channels that open during the respiratory burst are formed directly by components of NADPH oxidase. The data suggest that PMA stimulation modulates preexisting H^+ channels rather than inducing a new H^+ channel. (Supported by NIH grants HL52671 and A132041.)

72. Ionic Selectivity of Endogenous Hemi-gap Junction Currents Expressed in Polarized Epithelial Cells Isolated

from *Necturus* Urinary Bladder LEONCIO A. VERGARA,* MIGUEL J. LOPES,† MALCOLM BRODWICK,* and LUIS REUSS,* *Department of Physiology & Biophysics, University of Texas Medical Branch, Galveston, Texas; and †Federal University of Minas Gerais, Belo Horizonte, Brazil

Polarized epithelial cells isolated from *Necturus* urinary bladder express large linear currents activated by depolarization and decreases in external calcium ($[Ca^{+2}]_o$). The latter also results in increased uptake of small hydrophilic dyes. Gap-junction conduction blockers inhibit both phenomena (Vanoye et al. 1999. *Am. J. Physiol.* 276:C279–C284). In normal $[Ca^{+2}]_o$, as revealed by voltage-clamp and tail-current analysis, the conductance presents complex, slow activation kinetics, with a threshold near 0 mV. Lowering $[Ca^{+2}]_o$ shifts the voltage dependency to more negative values in a concentration-dependent manner (Lopes et al. 1999. *J. Gen. Physiol.* 114:22a). Here, we describe in detail the ionic selectivity of these currents. Studied in near symmetrical KCl-based solutions (pipette solution diluted 10%), the currents exhibited linear conductances with no rectification, as revealed by voltage ramps or rapid trains of short pulses applied from depolarized holding potentials (V_h). However, the observed reversal potentials (E_{rev}) were more positive than expected, and the difference increased in proportion to the magnitude of the depolarization. We interpreted the phenomenon as transitory changes in driving force due to current-dependent ionic accumulation. Dilution potential studies (At $V_h = 0$ mV and low $[Ca^{+2}]_o$) revealed a Cl:K⁺ selectivity of ~10:1, while bi-ionic studies revealed a lower permeability to organic anions (1:2 for cyclamate and 1:18 for aspartate, with respect to Cl). In spite of its selectivity, the striking similarity between the kinetic properties of this current and the hemichannels recorded upon Cx46 expression in oocytes (Ebihara et al. 1993. *J. Gen. Physiol.* 102:59-74), as well as those described in horizontal catfish retina (DeVries et al. 1992. *J. Physiol.* 445:201–230), supports the idea that functional GJH are expressed in epithelial cells. (Supported by NIH grant DK38734. M.J. Lopes was supported by CNPq, Brazil.)

73. Primary Culture of Porcine Vas Deferens Epithelial Cell Monolayers: A Novel System for Vectoral Ion Transport ROGER L. SEDLACEK, RYAN W. CARLIN, and BRUCE D. SCHULTZ, *Department of Anatomy and Physiology, Kansas State University, Manhattan, Kansas*

Vas deferens epithelia modulate the luminal fluid composition to provide the appropriate environment for sperm maturation, quiescence, and activation. Furthermore, epithelial function plays a key role in development or maintenance of the duct since cystic fibrosis, an inborn error in epithelial anion secretion, is almost universally associated with congenital bilateral absence of the vas deferens (CBAVD). Ion transport of the vas deferens from large mammals has not been widely studied due to the difficulty in obtaining suitable amounts of tissue for analysis and a tissue geometry that does not lend itself to traditional flux assays. Thus, a technique has been developed to establish monolayer cultures of freshly isolated porcine vas deferens epithelium. After recovery from a local slaughter house, excised vas deferens are flushed to remove residual ejaculate, filled with a collagenase-based dissociation solution, and closed. Incubation at 37°C, under the cover of a balanced salts solution, for 20–60 min, produced varying amounts of cells released from the epithelial lining of the lumen. Cells harvested from each tissue were then transferred to vented tissue culture flasks and grown in DMEM

supplemented with 10% fetal bovine serum and penicillin/streptomycin in a humidified 37°C incubator with a 5% CO₂ atmosphere. Flasks reached confluency in 3–5 d and were subsequently trypsinized and seeded onto permeable supports. Cultured cells displayed a monolayer cobblestone appearance and expressed cytokeratin, but not vimentin. Electron microscopy was employed to demonstrate the presence of junctional complexes and microvilli. When evaluated in modified Ussing chambers, cultured monolayers exhibited a high electrical resistance (>1,000 Ohm cm²) and responded to neurotransmitters with changes in short circuit current indicative of anion secretion. Attempts to further optimize culture conditions have shown that chronic exposure to steroid hormones modifies growth rates and ion transport characteristics. Thus, the culture method described will reliably produce viable neurotransmitter-responsive cell monolayers that will allow for the characterization of vas deferens epithelial function and associated control mechanisms. (Supported by the Cystic Fibrosis Foundation grant SCHULT99P0.)

74. Bicarbonate-dependent Ion Transport by Vas Deferens Epithelial Monolayers RYAN W. CARLIN, KATHY E. MITCHELL, ROGER L. SEDLACEK, and BRUCE D. SCHULTZ, *Department of Anatomy and Physiology, Kansas State University, Manhattan, Kansas*

Epithelial ion transport mechanisms have not previously been studied in the vas deferens of large mammalian species. Porcine vas deferens epithelial cells were isolated from adult animals and grown to confluence on permeable supports. Ion transport was evaluated in modified Ussing chambers, where initial results indicated that cultured cell monolayers exhibited high electrical resistance (>1,000 Ohm cm²) with little basal short circuit current (I_{sc} ; <1 μ A cm⁻²). Amiloride had no effect on I_{sc} . However, exposure to forskolin or selected neurotransmitters resulted in an increase in I_{sc} that is indicative of anion secretion. The response to forskolin was characterized by a transient peak ($\Delta I_{sc} = 4.2 \pm 0.5 \mu$ A cm⁻²) followed by a sustained plateau (ΔI_{sc} by the absence of HCO₃⁻ in the bathing media ($\Delta I_{sc} = 0.4 \pm 0.2 \mu$ A cm⁻²), although the transient peak was not significantly changed ($\Delta I_{sc} = 2.9 \pm 0.5 \mu$ A cm⁻²). A bumetanide-inhibitable component of forskolin-stimulated I_{sc} was present in HCO₃⁻-free conditions, but was absent in Cl⁻-free conditions. Cultured vas deferens epithelial cell lysates were resolved by SDS-PAGE and transferred to nitrocellulose membrane for immunodetection. When probed with an antibody raised against human carbonic anhydrase II, two bands of ~16 and 30 kD were detected. When probed with the same antibody, histological sections of native epithelial cells displayed diffuse cytoplasmic staining with slightly greater reactivity present in the subapical portion of the cells. When native tissue sections were probed with antibodies raised against an epitope of the sodium bicarbonate cotransporter (NBC a.a. 338–391), membrane-associated staining was observed. These results demonstrate that vas deferens epithelial cells possess the mechanisms necessary for the vectoral transport of bicarbonate and that these mechanisms are maintained in primary culture. Functional results indicate that vas deferens epithelia exhibit at least two anion-dependent cAMP-stimulated secretory processes with ongoing secretion requiring the presence of HCO₃⁻. (Supported by the Cystic Fibrosis Foundation grant SCHULT99P0.)

75. Gadolinium Effects on the Viability of Cultured Human Renal Proximal Tubule Epithelial Cells XIAOYONG

BAO, LEONCIO A. VERGARA, and LUIS REUSS, *Department of Physiology and Biophysics, University of Texas Medical Branch, Galveston, Texas 77555-0641*

We have previously shown that human renal proximal tubule (hPT) cells express gap-junctional hemichannels (GJH), which are most likely formed by Connexin 43 (Cx43). After short-term (≤ 1 h) ATP depletion to $\sim 50\%$, there is an increase in the uptake of 5/6-carboxyfluorescein (5/6CF, a fluorescent hydrophilic dye of MW 376) by confluent hPT cell monolayers. This effect can be blocked by the GJH-blocker gadolinium (Gd^{3+} , $10 \mu\text{M}$), suggesting that GJH are activated by metabolic inhibition. Furthermore, by using the propidium iodide (PI) exclusion assay immediately after the 5/6CF loading but in the presence of Gd^{3+} (to prevent PI uptake via GJH), we have found that short-term ATP depletion also results in an increase in the number of necrotic cells. When Gd^{3+} is added earlier and continuously present, both the 5/6CF uptake and the number of necrotic cells are reduced, suggesting that GJH activation is directly involved in the process of cell death. Preliminary data obtained by combining the FITC-annexin V and the PI exclusion assays show that ATP depletion to $\sim 20\%$ results in apoptosis after 12 h, whereas greater ATP depletion (to undetectable levels) induces massive cell necrosis in just 2 h. Using the LDH release test, we have found that long-term (≥ 12 h) metabolic inhibition results in an increase in the rate of necrosis in confluent cell monolayers, an effect that depends on the magnitude and duration of ATP depletion. In contrast to the short-term observations, prolonged exposure to Gd^{3+} during long-term ATP depletion further decreased the ATP levels and increased the percentage of necrotic cells, suggesting a slow toxic effect. Taken together, these results support the notion that activation of HGJ may play a role in epithelial cell death brought about by decreases in ATP levels. [Supported in part by the American Heart Association (National) grant 0050353.]

76. The Conduction Velocities of Calcium Action Potentials Are Highly Conserved LIONEL F. JAFFE, *Marine Biological Laboratory, Woods Hole, Massachusetts; and Brown University, Providence, Rhode Island*

Calcium waves are a major signaling mechanism within living systems. They have been put into four classes based on their velocities, which vary from a nanometer per second to nearly 100 cm/s (Jaffe. 1999. *Bioessays*. 21:657–667). The two best understood groups are: (a) fast calcium waves, which move at 10–30 $\mu\text{m/s}$ in fully active systems and are propagated by a reaction-diffusion mechanism; and (b) slow calcium waves, which move at 1–3 $\mu\text{m/s}$ and are thought to be mechanically propagated. Here this scheme is extended to calcium action potentials. These are here considered ultrafast calcium waves and prove to move at ~ 10 –50 cm/s wherever the velocity is limited by intracellular mechanisms. Such waves are, of course, electrically rather than chemically or mechanically propagated.

The supporting data were critically compiled from published observations of the velocities of calcium action potentials in the syncytial trabecular reticulum of a sponge (Leys et al. 1999. *J. Exp. Biol.* 202:1139–1150), in jellyfish and tunicate epithelia, in neurons within systems that range from jellyfish and sea urchins up to rat brains, in muscles within organisms that range from *Ascaris* to crabs and sheep and in the trap lobes of insectivorous plants. All of these waves move at ~ 10 –50 cm/s with no demonstrable relationship to cell width. This fivefold range contrasts sharply with that of the better known sodium action potentials whose velocities vary by a 1,000-fold in different systems and rise with cell width.

Conservation of velocity in the other three classes of (slower) calcium waves is attributed to propagation by molecular machines too complex to be effectively changed by random mutations. However, the machines that propagate action potentials consist of little more than voltage-sensitive ion channels within the plasma membrane. So maybe the invariant velocity of calcium action potentials is just the highest one that does not raise cortical calcium to toxic levels.

77. Potassium Accumulation by Nitella CHARLES BARR, *Department of Biological Sciences, State University of New York, Brockport, New York*

Isolated internodal cells of *Nitella* are not really ideal for studying the uptake of potassium. Only so much K can be accumulated and, as this level is approached, complex behavior may be expected. Spontaneous action potentials have been observed, perhaps serving to discharge the surplus K. In intact strands of *Nitella*, the cells near the growing point all have membrane potentials more electronegative than the K equilibrium potential; this is consistent with K accumulation. But isolated cells sometimes behave similarly, sometimes not. The present work involves some tactics whereby the opening and closing of the K channels may be evoked.

78. Simulations of Potassium Channel Function: KcsA and Homology Models MARK S.P. SANSOM, INDIRA H. SHRIVASTAVA, RICHARD J. LAW, and CHARLOTTE E. CAPENER, *Laboratory of Molecular Biophysics, University of Oxford, Oxford, United Kingdom* (Sponsor: Pamela Pappone)

Molecular dynamics simulations of a bacterial potassium channel (KcsA) embedded in a hydrated phospholipid bilayer (Shrivastava and Sansom. 2000. *Biophys. J.* 78:557–570) have been used to explore the physical basis of ion permeation of K^+ ions and of the selectivity of this channel for K^+ over Na^+ ions. Comparison of simulations starting with either two K^+ ions (separated by a water molecule) or with two Na^+ ions plus a water molecule in the filter reveals significant differences in ion/protein interactions. K^+ ions and water within the filter undergo a concerted single file motion in which ions and water molecules translocate between adjacent “sites” within the filter. Such translocation occurs in both directions (extracellular to intracellular and vice versa) along the filter. By contrast, Na^+ ions remain bound to their sites within the filter without significant motion on a nanosecond timescale. Also, entry of a K^+ ion into the filter from the extracellular mouth has been observed, whereas this does not occur for a Na^+ ion. Furthermore, whereas K^+ ions sit within a cage of eight oxygen atoms of the filter, Na^+ ions prefer to interact rather more closely with a ring of four oxygen atoms. The simulations also reveal that the selectivity filter exhibits a significant degree of flexibility in response to changes in ion/protein interactions. Simulations have also been performed for a homology model of the pore-forming domain of Kir6.2 (Capener et al. 2000. *Biophys. J.* In press). The interactions of the Kir6.2 channel model with K^+ ions and water through the selectivity filter occur in a similar manner to that observed in simulations of KcsA. This suggests that such a single-filing mechanism is conserved between different K channel structures and is robust to changes in simulation details. As with KcsA, the Kir6.2 simulations suggest a degree of flexibility in the filter. (Supported by the Wellcome Trust.)

